ANNUAL REPORT

on

THERMAL MODELING WITH INTERNAL GENERATION

Report Prepared By

Dr. D. Maples
Mr. J. V. Scogin
Department of Mechanical and
Aerospace Engineering
College of Engineering
Louisiana State University
Baton Rouge, Louisiana 70803

ANNUAL REPORT

on

THERMAL MODELING WITH INTERNAL GENERATION

Report Prepared By

Dr. D. Maples
Mr. J. V. Scogin
Department of Mechanical and
Aerospace Engineering
College of Engineering
Louisiana State University
Baton Rouge, Louisiana   70803

This Report Prepared By:

D. Maples, Assistant Professor
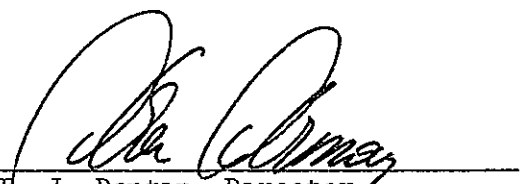Mechnical Engineering

This Report Approved By.

for H. J. Dantin, Director
Division of Engineering Research

TABLE OF CONTENTS

LIST OF SYMBOLS

A_s — Surface area, (sq. in.)

BTU — British Thermal Unit

C_p — Specific heat (BTU/lb.°F)

D — Diameter (in.)

I — Current (amps)

k — Thermal conductivity (BTU/hr.ft.°F)

L — Length (in.)

p — Power (watts)

q'' — Heat radiated at surface (BTU/hr.sq.in.)

q_{gen} — Heat generated per unit volume (BTU/hr.cu.in.)

q — Heat transfer rate (BTU/hr.)

$\dot{q}$ — Heat transfer rate per unit area (BTU/hr.sq.in.)

r — Radius at any point in rod (in.)

R — Outside radius of rod (in.)

Res — Resistance (ohms)

R_{rf} — Arbitrary reference radius (in.)

T — Temperature (°F)

T_R — Temperature at surface of rod at any time (°F)

t — Time (min.)

T_{rf} — Arbitrary reference temperature (°F)

V — Volume (cu.in.)

LIST OF SYMBOLS (cont'd)

Greek Symbols

α Absorptance

ϵ Emmittance

σ Stefan-Boltzmann constant (0.1712×10^{-8}) BTU/sq.ft.-hr.-°R^4)

ρ Density (lb/cu.ft.)

ρ_e Electrical Resistivity (ohms-ft.)

Subscripts

o Reference or constant value

m Model

p Prototype

s Surface

L Lead

R Rod

rf Reference Value

LIST OF FIGURES

LIST OF TABLES

CHAPTER I

INTRODUCTION

The prediction of temperatures and temperature gradients within a spacecraft while it is operating in a space environment has become a significant problem in the design of such spacecrafts. Performance tests on full sized prototypes of the spacecraft in a simulation chamber were first used to solve this problem but the advent of extremely large spacecrafts and space stations has made this technique become outmoded. As a result, thermal modeling has reached a level of increasing importance, since it can successfully be used to predict the thermal behavior of a spacecraft from model test data.

A great abundance of analytical and experimental work has been done in the area of thermal modeling for steady state conditions imposed on conduction-radiation coupled systems in recent years. The transient behavior of thermal models has been greatly neglected, however, and the need for more work in this area is readily apparent.

The primary objective of this investigation was to develop a practical method for thermal modeling of a conduction-radiation design under transient conditions. The design selected for this investigation consisted of solid rods. The models and prototypes were tested in a cold, high-vacuum environment. Simulated solar or particle radiation was not attempted.

CHAPTER II

LITERATURE SURVEY

In 1962 the results of thermal modeling of spacecraft and their com-
ponent parts began to appear in the literature. Vickers (1) published a
literature review of thermal modeling efforts covering the years 1962-1965.
Vickers emphasized that while many text and papers on thermal similitude
and modeling had been written, most of these mainly concerned modeling of
convective problems and payed little or no attention to the modeling of
conduction or radiative situations. This is indeed unfortunate since coupled
conduction and radiation predominates in spacecraft.

Vickers discussed two basic methods of thermal modeling The first
method was "temperature preservation", where the model and prototype abso-
lute temperatures are equal. In the "material preservation" method the
model and prototype are constructed of the same material. Vickers concluded
that the two methods were mutually exclusive, assuming perfect geometric
similarity between the model and prototype. The article also discussed
general problems of thermal modeling, reasons for improving the state-of-
the-art, and advantages to be derived therefrom.

As Vickers stated, the first paper in the area of spacecraft thermal
modeling was by S. Katzoof (2). Katzoof derived five dimensionless groups
from dimensional analysis, and the major portion of his paper was devoted
to the practical problems in using the groups he presents. The groups
Katzoof derived were concerned with radiation, internal heat generation,
thermal conductivities of materials, heat capacities of materials, and

2

joint conductance. The five parameters were:

$$\frac{\sigma T^4}{q} \ , \quad \frac{qL}{q} \ , \quad \frac{qL}{kT} \ , \quad \frac{c_\rho LT}{q \ \theta} \ , \quad \text{and} \quad \frac{CL}{k} \tag{1}$$

The last ratio in equation (1) applies to joint conductance. This group
of ratios does not explicitly include radiation exchange between surfaces;
however, they form an independent group. If joint conductance is neglected,
equation (1) becomes:

$$\frac{CT^4}{q} \ , \quad \frac{c_\rho LT}{q \ \theta} \ , \quad \frac{q \ L}{k \ T} \ , \quad \text{and} \quad \frac{q \ L}{q} \tag{2}$$

In 1962, A. J. Katz (3) discussed very briefly the criteria involved
in thermal scale modeling, and some of the problems which might be involved.
Katz, Clark, and Leband (4) were the first investigators to use dimensional
analysis for establishing the thermal modeling criteria in space applications,
and a very detailed paper was presented by this group. They derived a group
of dimensionless ratios used to study the temperature of composite wall
constructions exposed to an external radiation environment. Leband and
Clark presented the ratios in equation (3)

$$\frac{\sigma T^4}{q} \ , \quad \frac{qL}{kT} \ , \quad \frac{c_\rho L^2}{k\theta} \tag{3}$$

and Katz presented the ratios in equation (4)

$$\frac{\sigma T^3 L}{k} \ , \quad \frac{qL^2}{k \ T} \ , \quad \frac{c_\rho L^2}{k \ \theta} \tag{4}$$

3

The two groups of ratios in equations (3) and (4) may be combined to form
equation (5):

$$\frac{qL^2}{k\,T}\,, \quad \frac{qL}{kT}\,, \quad \frac{\sigma T^3 L}{k}\,, \quad \frac{c_\rho L^2}{k\,\theta}\,, \quad \text{and} \quad \frac{\sigma T^4}{q} \tag{5}$$

The ratios in equation (5) that form an independent group are

$$\frac{\sigma T^3 L}{k}\,, \quad \frac{c_\rho L^2}{k\,\theta}\,, \quad \frac{d\,L}{k\,T}\,, \quad \text{and} \quad \frac{q\,L^2}{k\,T} \tag{6}$$

If joint conductance were neglected, equation (1) would become

$$\frac{cT^4}{q}\,, \quad \frac{c_\rho LT}{q\,\theta}\,, \quad \frac{qL}{kT}\,, \quad \text{and} \quad \frac{d\,L}{q} \tag{7}$$

Equations (6) and (7) are not identical groups of independent ratios,
although they apply to the same physical problem. Either of the groups
may be derived from the other.

Wainwright, Kelly, and Keesee (5) discussed the development of dimen-
sionless groups from both a dimensional analysis approach and from a dif-
ferential equation approach. The similarity groups obtained were as
follows:

$$\frac{k_o\,\theta_o}{P_o c_{po} L^2}\,, \quad \frac{\sigma \varepsilon L^2 T_o^3}{k_o(\Delta R)}\,, \quad \frac{q}{\sigma \varepsilon T_o^4} \tag{8}$$

Hrycak and Unger (6) developed the same thin shell thermal modeling criteria
that are presented in equation (8) when the system is referred to in spherical
coordinates. Such prototypes as Telstar were modeled by these investigations.

In dimensional analysis the pertinent variables are identified at the outset. Some insight into the problem and knowledge of at least one combination of parameters are considered essential to the success of this method. The entire group of dimensionless combinations of these parameters formulates the modeling criteria.

The similitude approach consists of writing the governing differential equation for the model and prototype thermal behavior. The model equation is identical to the prototype equation if the dimensional elements multiplying corresponding terms are identical in value. The modeling criteria are established by equating the ratios of corresponding dimensional multiplying elements in the model and the prototype differential equations.

B. P. Jones (7) and (8) used the differential equations which described the thermal behavior of a spacecraft to derive the similarity parameters of thermal modeling. Jones developed twenty-eight dimensionless ratios that had to be constant from prototype to model if complete similarity was to exist. All of the ratios were not independent, but it was possible to find seven independent groups of ratios. A comparison of his resulting similarity parameters with those of Vickers and other investigators was made by Jones and the results were found to be the same.

Chao and Wedekind (9) assumed a relationship between thermal conductivity and temperature, ignoring only polarization and assuming incoherency of the light, and in their approach state the necessary and sufficient conditions for modeling real surfaces under any form of solar input or simulation. They introduced the concept of using a power law function of temperature for specific heat and thermal conductivity and also discussed the possibility of the model not being geometrically similar

5

to the prototype.

Fowle, Gabron, and Vickers (10) made an elaborate attempt at scale modeling in order to predict the temperature of the Mariner IV spacecraft. The Mariner IV was exposed only to external radiation from the sun, and was at a fixed altitude with respect to the sun. This allowed steady state modeling to be applied. A prototype, which simulated the basic features of the Mariner spacecraft, was built and was then modeled at one-half and one-fifth scales using the the temperature-preservation technique and at one-half scale using the materials preservation technique. Reasonable success was obtained with all three models; that is, discrepancies between model and prototype were, in almost all cases, accounted for. The models were tested at steady state with cold-wall and high-vacuum conditions.

In 1963 Vickers (11) again discussed the techniques which could be evolved from the basic laws of thermal scale modeling of spacecraft. The equations presented for the similarity parameters by Vickers in this article agreed with those developed by Fowle, Gabron, and Vickers, Jones, and earlier writers. The dimensionless groups were.

$$\frac{qL^2}{kT} , \frac{\rho c_\rho L^2}{k\theta} , \frac{\epsilon \sigma T^3 L}{k} , \frac{CL}{k} , \frac{\alpha_{kj} \phi_{jk} L}{kT} , \frac{\alpha_s SL}{kT} , \frac{q}{LkT} , \frac{qL}{kT} \qquad (9)$$

If q, q, and q are considered as distinct physical quantities, equation (9) forms one group of independent ratios. The first ratio and last two ratios listed in equation (9) may be reduced to one by introducing the relations $q = q/L^2$ and $q = q/L^3$. The resulting group contains six independent ratios which includes one for joint interface conductance. In this case q is

6

a characteristic power; however, in certain modeling it may be desirable to consider q, q, and q as distinct quantities.

In 1964 a paper by J. R. Watkins (12) revealed that he had developed forty-nine groups, each of which contained seven independent similarity ratios for the general case of thermal modeling. Watkins used the dimensional analysis approach to develop similarity ratios. By defining the energy transfer to and from single, elemental, isothermal volumes of the prototype and model in a simulated space environment, Watkins was able to use the computer to derive his similarity ratios. A numerical approach to dimensional analysis was also applied to the physical quantities that describe the thermal behavior of two radiating disks connected by a conducting rod. The numerical solution yielded fifty-seven groups each of which contained five independent ratios. Any one of these groups may be used for model design, the selection depending upon what is to be the purpose of the model experiments.

Matheny (13) was one of the earlier investigators to conduct experiments that involved transient thermal modeling. For his system Matheny chose two disks connected by a conducting member. The conducting member was made large enough to enter into radiant interchange. The models were designed according to the criteria

$$\frac{\sigma T^3 L}{k} \; , \quad \frac{c_\rho L^2}{k\theta} \; , \quad \frac{qL}{kT} \; , \quad \text{and} \; \frac{qL^2}{kT} \tag{10}$$

The results of the transient tests which were conducted on the prototype and one-half scale model were excellent.

The modeling criteria given by equation (8) were applied to a conceptual space station by Folkman, Baldwin, and Wainwright (14). Geometric scaling was used and external radiation sources were preserved. The experimental results obtained from tests performed on the model were compared with three-dimensional transient analysis.

R. E. Rolling (15) and (16) developed modeling criteria for space vehicles by using the similitude approach. Rolling's procedure was identical to that of Chao and Wedekind. The criteria in equation (11) were developed for prediction of prototype behavior from model behavior for a radiation-conduction coupled problem, where the "starred" terms represent the ratio of model to prototype properties.

$$\frac{\rho^* V^* c_\rho^* T^*}{\theta^*} = A_s^* \, S^* \, F_s^* = A_r^* \, R^* \, F_r^* = A_e^* \, E^* \, F_e^*$$

$$= q^* = k_n^* \, A_n^* \, \frac{(T^*)}{X^*} = A_j^* \, F_j^* \, T^{*4} \tag{11}$$

The criteria in equation (11) were used to model two opposed disk with four connecting tubular members and truncated cones.

Rolling used one-half and one-quarter scale models in his tests, and fixed material thermophysical properties while temperature and time were scaled. Geometric distortion in the minor dimensions was permitted. Arrays of tungsten filament lamps were used for external radiation sources. The results for the opposed connected disks and for the cones proved that the criteria in equation (11) were reasonably accurate for modeling purposes. The temperatures of the model for the disks were
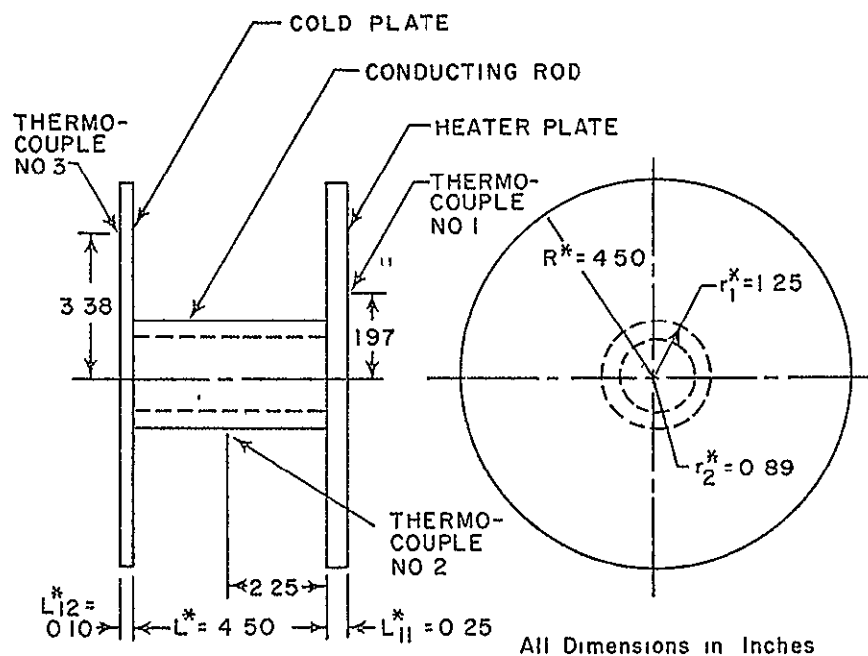
8

within 9°K of the prototype, and for the cones all model temperatures were within 8°K of the prototype.

Young and Shanklin (17) modeled a system composed of three sections· a heater plate containing an electrical resistance heating element which represented an internal energy source of variable strength, a cold-plate having no internal energy source, and a cylindrical rod connecting the two plates. The ratios in equation (12) were applied to this system.
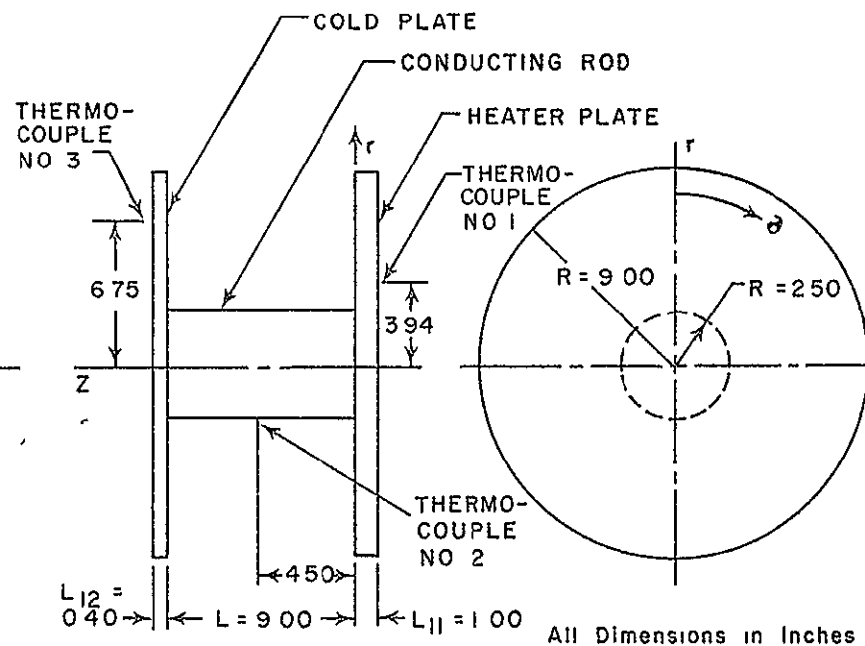
$$\frac{R^2}{L_z} \, , \quad \frac{R^2 F_{i-j}}{L_z} \, , \quad qR^2 , \quad \frac{R_r}{R} \, , \quad \frac{R_r R}{L_z L} \, , \quad \frac{\theta}{R^2} \, , \quad \frac{L^2}{R_r} \, , \quad \text{and} \quad \frac{L^2 F_{i-j}}{R_r} \tag{12}$$

The prototype and the one-half scale model were fabricated of the same material with identical values of ε and α. The prototype and the model were exposed to identical simulated space conditions and were started at the same initial temperature, T_{10}. Furthermore, the prototype and model surfaces were blackened such that ε and α approached unity. The ratios in equation (12) were used in designing the model. The system used and a large portion of the results of the investigation are shown in Figure 1 and Figure 2, respectively. Model temperatures deviated from those of the prototype by an average of approximately 1.5 percent.

Gabron and Johnson (18) submitted a report to the Jet Propulsion Laboratory describing their work on thermal modeling of the Mariner Mars 64 spacecraft. A forty-three hundredth scale model of the spacecraft was fabricated and tested under steady-state thermal conditions. The "temperature preservation" technique was employed, with no solar radiation.

COLD PLATE

CONDUCTING ROD

HEATER PLATE

THERMO-COUPLE NO 3

THERMO-COUPLE NO I

3 38

197

$R^* = 4 50$

$r_1^* = 1 25$

$r_2^* = 0 89$

THERMO-COUPLE NO 2

$L_{12}^* = 0 10$

$L^* = 4 50$

$2 25$

$L_{11}^* = 0 25$

All Dimensions in Inches

MODEL GEOMETRY

COLD PLATE

CONDUCTING ROD

HEATER PLATE

THERMO-COUPLE NO 3

THERMO-COUPLE NO I

r

6 75

3 94

r

$R = 9 00$

$R = 2 50$

∂

Z

THERMO-COUPLE NO 2

$L_{12} = 0 40$

$L = 9 00$

$4 50$

$L_{11} = 1 00$

All Dimensions in Inches

PROTOTYPE GEOMETRY

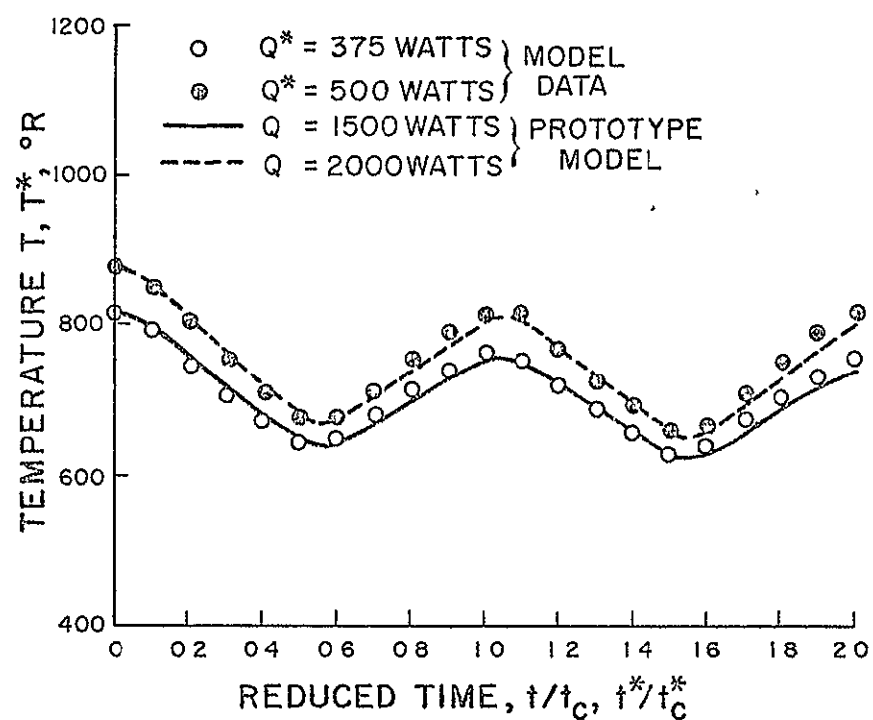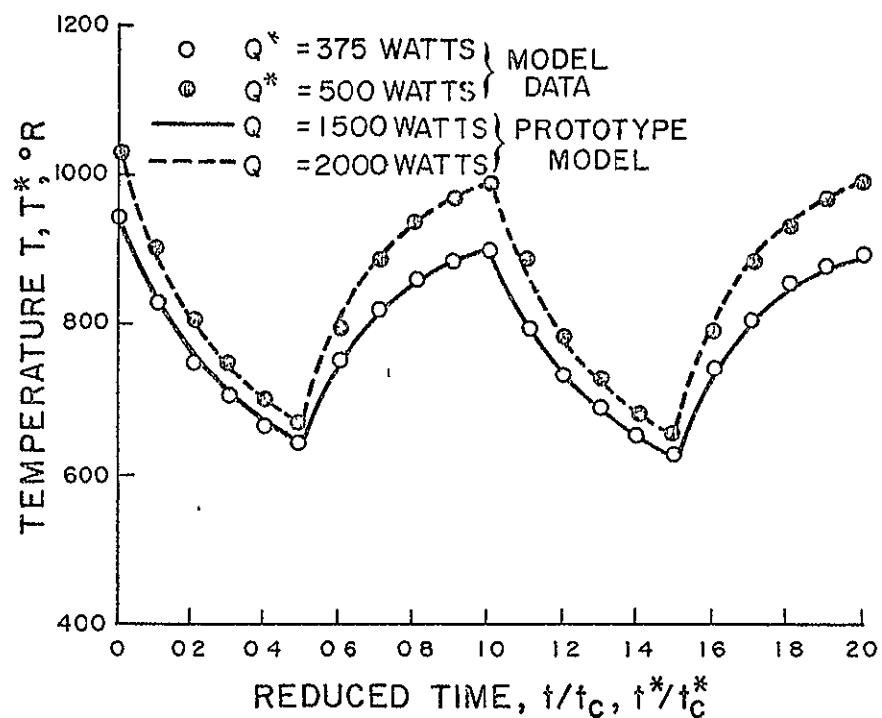FIGURE I   SPOOL CONFIGURATION   (SOURCE· REF 17)

FIGURE 2   TEMPERATURE - TIME CHARACTERISTICS OF THE SYSTEM
SHOWN IN FIGURE 1 (SOURCE: REF. 17)

It was concluded that "temperatures within a complex spacecraft structure, typical of the Mariner vehicle, can be predicted by use of 'temperature preservation' thermal-scale modeling techniques to an accuracy useful for the verification of thermal design concepts."

Jones and Harrison (19) used the group of ratios given in equations (13) and (14) to model a system composed of a plate, cylinder, and sphere which were exchanging thermal energy by radiation only.

$$\frac{T_j}{T_k}, \quad \frac{E_{kj} F_{kj} A_k}{E_j A_j}, \quad \frac{\alpha_j^S A_j S\theta}{\bar{c}_j T_j} \tag{13}$$

$$\frac{E_j \sigma A_j T_j^3 \theta}{\bar{c}_j}, \quad \frac{c_{kj} \theta}{\bar{c}_j}, \quad \text{and} \quad \frac{q_j \theta}{\bar{c}_j T_j} \tag{14}$$

Electrical resistance heaters were used to obtain the simulated heating effects of the sun, and the space chamber was regarded as incorporated in the ratio involving radiative interchange between surfaces. Equations (13) and (14) then reduce to

$$\frac{T_j}{T_k}, \quad \frac{R_{kj} T_j^3 \theta}{\bar{c}_j}, \quad \frac{q_j \theta}{\bar{c}_j T_j} \quad (j, k = 1, \ldots, n_j \, k \neq j) \tag{15}$$

The materials were not changed from prototype to model, the radiation geometry factors were assumed to remain unchanged, the temperatures of the model at a particular time were assumed to be equal to the corresponding prototype temperatures at the same time, and the thickness of the cylinder end caps was not changed from prototype to model. The major external dimensions were scaled by one-half. The experimental results generally

confirmed the modeling rules.

Adkins (20) introduced a method of geometric scaling which made thermal modeling possible while preserving both material and temperature. The Fourier conduction equation with radiation boundary conditions was used to establish the similarity criteria for two different configurations, a nonconduction array and a conduction array. The similarity ratios were

$$\frac{L^2 \rho c_\rho}{k \theta_o} \, , \quad \frac{L}{d}, \quad (\sigma T_o^3 \, d)/k \tag{16}$$

In 1966, Miller (21) investigated the applicability of thermal modeling to steady-state and transient conduction in cylindrical solid rods, for both single and multiple material systems. By performing a similitude analysis, Miller obtained the following relations:

$$q^* = L^{*-2}, \quad q^* = L^{*-1}, \quad q^* = L^{*3}, \quad T^* = 1, \quad \theta^* = L^{*2}, \quad R^* = L^{*2} \tag{17}$$

where the starred quantities again represent the model to prototype ratio of the parameter.

Shih (22) presented a discussion of thermal modeling which included the presentation of some of the same similiarity parameters as Miller. He took into account changes of thermal conductivity and specific heat with temperature and included the geometric relationship $R^* = L^{*2}$ for preserving both material and temperature in model and prototype. No experimental work was presented or planned, nor was there any reference to joined materials with different thermal properties.

Price (23) investigated a model that maintained both material and

13

temperature preservation at homologous locations. The prototype and model, which were built and tested, were cylindrical fins. Also, mathematical models of the prototype and model were solved using the computer. The similarity criteria used were those developed by Miller. Experimental results showed that the scaling laws were valid. Also the theoretical data agreed with enough accuracy to validate using the mathematical model, when the model is simple.

Summary

Analytical and experimental research in thermal similitude in space-related thermophysics problems was very active from 1962 to 1966, but has become somewhat inactive since 1966. However, a rejuvenation of this research occurred in 1968, and more emphasis is being placed on thermal modeling endeavors. Much progress has been made in confirming the analyses by experiments in both steady-state and transient cases. However, more work is needed in the conduction-radiation area with emphasis on transient problems. There is also a great need for verification of a group of similarity parameters for a system containing a fluid.

CHAPTER III

MODELING CRITERIA

The obvious objective of thermal scale modeling is to maintain thermal similitude between a prototype and model. This is achieved by preserving the numerical equality of certain dimensionless groups of properties of the prototype and model. These thermal similarity parameters may be identified from either dimensional analysis or from dependence upon the differential equations describing the thermal behavior of the model and/or prototype. For the inexperienced, the latter method of using the differential equations and boundary conditions is much more desirable. However, either method will result in the same set of similarity parameters.

The modeling criteria for the models and prototypes considered in this investigation were developed using the differential method. This technique was found in the reference by Murrill, Pike, and Smith (25) and was employed in getting the similarity parameters. Before proceeding to the derivations of the parameters, some discussion is in order concerning the constraints placed on the problem to facilitate the derivation process.

The first restriction was that the materials used be homogeneous and isotropic. The second basic assumption was that there be perfect geometric similarity between prototype and model. Third, to eliminate the influence of spectral and angular distribution on the emitted radia-

tion, it was assumed that the prototype and model had the same uniform
and constant surface characteristics. To assure control of the third
constraint, the surface of the prototypes and models was coated by a
flat black velvet paint, which in turn assured the emissivity and
absorptivity of the surfaces be constant and independent of temperature.
It was also assumed that the radiant heat flux from a simulated space
environment is approximately zero, which is a safe assumption if solar
energy is not simulated and the temperature approaches absolute zero.
As a consequence of the fourth assumption, it was also assumed that all
energy radiated from the models and prototypes was absorbed by the walls
of the cryogenic liner inside the simulation chamber. A fifth assumption
was that thermal properties of the model and prototype were constant and
did not vary during a test run. To assure this, a temperature range of
approximately thirty to ninety degrees Fahrenheit was used during all of
the test runs. Finally, heat transfer due to convection was assumed to
be negligible, which is an excellent assumption in a vacuum environment.

With these constraints in mind, the decision was made to test titan-
ium and stainless steel rods to verify the modeling criteria for a con-
duction-radiation problem. These rods were very long relative to diameter
for the purpose of minimizing end effects. The technique found in re-
ference (25) was used to develop the similarity parameters.

In order to derive the similarity parameters needed for thermal scale
modeling, it is necessary to make appropriate changes of variables in the
describing differential equation. A step-by-step technique was presented
by Murrill, Pike and Smith for making the correct changes of variables

for two basic reasons. First, those inexperienced in the field could

use this technique to derive the proper changes of variables. Second,

this systematic technique could be used for problems in which the proper

changes of variables are not obvious. Normally, the changes of variables

are made for the dependent and independent variables in order to reduce

the number of groups of parameters required to adequately describe the

problem. However, in a few cases the changes of variables are even more

helpful. Sometimes the number of independent variables required in the

equations can be reduced, such changes in the independent variables being

known as similarity transforms. The derivation of similarity transforms

is a degree more difficult than the derivation of changes of variables,

but the technique presented will obtain such similarity transforms, if

they exist, in addition to changes of variables.

The techniques for reducing the number of parameters or dimensionless

groups required to mathematically describe a physical problem have been

investigated for many years. The description of problems using the mini-

mum number of parameters is the subject of such apparently diversified

fields as dimensional analysis, inspectional analysis, and scale-up theory.

However, these techniques typically consider only changes of variable,

and not similarity transforms. Since the following technique applies to

similarity transforms as well, it would seem to be preferable.

The basic steps in this method of analysis are as follows:

1. Introduce arbitrary reference quantities in order to place

   the dependent and independent variables in dimensionless form.

   This typically takes the following form:

18

$$\frac{\text{variable-arbitrary reference value}}{\text{arbitrary reference difference}}$$

For example, the temperature T may be non-dimensionalyzed as $(T-T^*)/\Delta T^*$, where T^* is some arbitrary reference value and ΔT^* is some arbitrary characteristic temperature difference in the problem.

2. Introduce these changes of variable into the differential equations and their boundary conditions, rearranging as necessary so that the parameters appear in dimensionless groups.

3. Equate each dimensionless parameter containing an arbitrary reference quantity to either unity or zero until all arbitrary constants have been defined.

In the third step a system of algebraic equations is obtained that relate the arbitrary constants to the original parameters of the problem. There are three possibilities for this set of algebraic equations.

1. More equations than unknowns, i.e., an overdetermined set of equations. In this case there will be groups of parameters or dimensionless groups remaining in the transformed equations.

2. Number of equations equals number of unknowns. For such situations no dimensionless groups of parameters usually remain in the transformed equations.

3. Fewer equations than unknowns, i.e., an undetermined set. In this case, a similarity transform is possible.

Derivation of Similarity Parameters

The general heat-conduction equation governing the temperature distribution and the conduction heat flow in a solid cylindrical system

19

having uniform physical properties is given by Kreith (26) as,

$$\frac{\partial^2 T}{\partial r^2} + \frac{1}{r} \frac{\partial T}{\partial r} + \frac{q_{gen}}{k} = \frac{\rho c}{k} \frac{\partial T}{\partial t} \qquad (18)$$

where q_{gen} represents internal generation due to resistance heating, and is equal to $\frac{I^2 (Res)}{V}$. The initial and boundary conditions for the rod in a low temperature vacuum environment are as follows:

$$T(r,o) = T_o \qquad (19)$$

$$\frac{\partial T(o,t)}{\partial r} = 0 \qquad (20)$$

$$-k \frac{\partial T(R,t)}{\partial r} = \sigma\varepsilon \left[T(R,t) \right]^4 \qquad (21)$$

The following dimensionless reference quantities will be introduced into equation (18) and the initial and boundary condition equations.

$$T^* = \frac{T - T_{rf}}{\Delta T_{rf}} \qquad (22)$$

$$r^* = \frac{r - r_{rf}}{\Delta r_{rf}} \qquad (23)$$

$$t^* = \frac{t - t_{rf}}{\Delta t_{rf}} \qquad (24)$$

Equations (22), (23), and (24) may be rearranged to give.

$$T = T^* \Delta T_{rf} + T_{rf} \qquad (25)$$

$$r = r^* \Delta r_{rf} + r_{rf} \qquad (26)$$

$$t = t^*\Delta t_{rf} + t_{rf} \tag{27}$$

The partial derivative of each of the above equations may next be found.

$$\frac{\partial T}{\partial r} = \frac{\Delta T_{rf}}{\Delta r_{rf}} \frac{\partial T^*}{\partial r^*} \tag{28}$$

$$\frac{\partial^2 T}{\partial r^2} = \frac{\Delta T_{rf}}{(\Delta r_{rf})^2} \frac{\partial^2 T^*}{\partial r^{*2}} \tag{29}$$

$$\frac{\partial T}{\partial t} = \frac{\Delta T_{rf}}{\Delta t_{rf}} \frac{\partial T^*}{\partial t^*} \tag{30}$$

Equations (28), (29), and (30) may be substituted into equation (18) and into the initial and boundary condition equations. Substitution into equation (18) gives:

$$\frac{\partial^2 T^*}{\partial r^{*2}} + \left(\frac{1}{r^* + \frac{r_{rf}}{\Delta r_{rf}}}\right)\frac{\partial T^*}{\partial r^*} + \frac{q_{gen}}{k}\frac{(\Delta r_{rf})^2}{\Delta T_{rf}} = \frac{\rho c}{k}\frac{(\Delta r_{rf})^2}{\Delta t_{rf}}\frac{\partial T^*}{\partial t^*} \tag{31}$$

Substitution into the initial and boundary condition equations (19), (20), and (21) gives the following results·

$$T^*\left(r^*, -\frac{t_{rf}}{\Delta t_{rf}}\right) = \frac{T_o - T_{rf}}{\Delta T_{rf}} \tag{31a}$$

$$\frac{\partial T^*\left[\left(-\frac{r_{rf}}{\Delta r_{rf}}, t^*\right)\right]}{\partial r^*} = 0 \tag{32}$$

21

$$\frac{\partial T^* \left(\frac{R-r_{rf}}{\Delta r_{rf}}, t^*\right)}{\partial r^*} = -\frac{\sigma\varepsilon(\Delta r_{rf})(\Delta T_{rf})^3}{k}\left[T^*\left(\frac{R-r_{rf}}{\Delta r_{rf}}, t^*\right) + \frac{T_{rf}}{\Delta T_{rf}}\right]^4 \qquad (33)$$

The dimensionless groups appearing in equations (31) through (33) are as follows:

$$\frac{r_{rf}}{\Delta r_{rf}} \qquad (34)$$

$$\frac{q_{gen}}{k}\frac{(\Delta r_{rf})^2}{\Delta T_{rf}} \qquad (35)$$

$$\frac{\rho c}{k}\frac{(\Delta r_{rf})^2}{(\Delta t_{rf})} \qquad (36)$$

$$\frac{t_{rf}}{\Delta t_{rf}} \qquad (37)$$

$$\frac{T_o - T_{rf}}{\Delta T_{rf}} \qquad (38)$$

$$\frac{R - r_{rf}}{\Delta r_{rf}} \qquad (39)$$

$$\frac{T_{rf}}{\Delta T_{rf}} \qquad (40)$$

$$-\frac{\sigma\varepsilon(\Delta r_{rf})(\Delta T_{rf})^3}{k} \qquad (41)$$

22

Since there are eight dimensionless groups in equations (34)
through (41), eight algebraic equations could be obtained of all these
groups were set equal to zero or unity. However, this would be an over-
determined set. There are six arbitrary constants; so, only six of the
groups can be selected.

The process of selecting the six groups is not as arbitrary as it
might seem. The following reasoning was used to obtain the changes
of variable

1. The term t_{rf} appears only in equation (37) and was set equal to
   zero to get the simplest form of equation (24).

2. The term T_{rf} appears in equations (38) and (40), and setting
   either of these equations equal to unity would complicate equation
   (22). Equation (40) was set equal to zero so that $T_{rf} = 0$.
   Setting equation (38) equal to zero would have given $T_{rf} = T_{o}$,
   and this too is suitable since T_{o} was the same for model and
   prototype.

3. The r_{rf} term appears in equations (34) and (39). Equation (34)
   was set equal to zero, which made $r_{rf} = 0$. This gave the simplest
   form of equation (23).

4. Equation (39) was set equal to zero, which gave $\Delta r_{rf} = R$. This
   is the simplest form that can be derived for Δr_{rf}, and it quarantees
   the presence of the rod radius in terms of R in the similarity
   parameters.

5. Equation (36) is the only group in which Δt_{rf} appears; so, this
   group was set equal to unity to define Δt_{rf}.

23

6. Equation (35) was set equal to unity to define ΔT_{rf} and to make

sure that the generation term appeared in the parameters. Power

predictions for a prototype based on experimental power measure-

ments from a model were used to achieve homologous temperatures

between models and prototypes; so, it was indeed necessary to

have a term for power (and in turn for generation) appear in the

similarity parameters.

This completed the selection of the six groups, and also the choice of

whether to set each equal to zero or unity.

At this point, then, the following expressions must hold:

$$\frac{t_{rf}}{\Delta t_{rf}} = 0 \tag{42}$$

$$\frac{T_{rf}}{\Delta T_{rf}} = 0 \tag{43}$$

$$\frac{r_{rf}}{\Delta r_{rf}} = 0 \tag{44}$$

$$\frac{R - r_{rf}}{\Delta r_{rf}} = 0 \tag{45}$$

$$\frac{\rho c}{k} \frac{(\Delta r_{rf})^2}{\Delta t_{rf}} = 1 \tag{46}$$

$$\frac{q_{gen}}{k} \frac{(\Delta r_{rf})^2}{\Delta T_{rf}} = 1 \tag{47}$$

Solving equations (42) through (47) for the six unknown reference quantities gives.

$$t_{rf} = 0 \tag{48}$$

$$T_{rf} = 0 \tag{49}$$

$$r_{rf} = 0 \tag{50}$$

$$\Delta r_{rf} = R \tag{51}$$

$$\Delta t_{rf} = \frac{\rho c R^2}{k} \tag{52}$$

$$\Delta T_{rf} = \frac{q_{gen} R^2}{k} \tag{53}$$

Substitution of equations (49) and (53) into equation (22) will satisfy the requirement of $T_m = T_p$ at homologous times.

$$T^* = \frac{T \ k}{q_{gen} \ R^2} \tag{54}$$

For point to point similarity to exist between model and prototype. equation (55) must hold.

$$\left(\frac{T \ k}{q_{gen} \ R^2} \right)_m = \left(\frac{T \ k}{q_{gen} \ R^2} \right)_p \ . \tag{55}$$

$$\frac{T_m}{T_p} = \left(\frac{k}{q_{gen} R^2}\right)_p \quad \left(\frac{q_{gen} R^2}{k}\right)_m \tag{56}$$

For equal thermal conductivities (model and prototype made of some material) and $q_{gen} = (I^2 Res/\pi R^2 L)$,

$$\frac{T_m}{T_p} = \left(\frac{I^2 Res}{L}\right)_m \quad \left(\frac{L}{I^2 Res}\right)_p \tag{57}$$

Since $T_m/T_p = 1$ is required, equation (58) must hold:

$$\left(\frac{I^2 Res}{L}\right)_m \quad \left(\frac{L}{I^2 Res}\right)_p = 1 \tag{58}$$

$$I_p = I_m \sqrt{\frac{Res_m/L_m}{Res_p/L_p}} \tag{59}$$

Equation (59) was convenient to use during the experiment to predict the current settings needed for prototypes. Equal starting temperatures and ending temperatures were achieved for models and prototypes using equation (59). The approach, then was to check the scaling technique by using power predictions to achieve temperature equality. Of course, a time scaling factor was required in plotting temperature versus time curves for models and prototypes to prove that temperature equality had been

26

achieved at any instant in time.

Substitution of equations (48) and (52) into equation (24) gave the time scaling equation between models and prototypes.

$$t^* = \frac{tk}{\rho c R^2} \tag{60}$$

$$\left(\frac{tk}{\rho c R^2}\right)_m = \left(\frac{tk}{\rho c R^2}\right)_p \tag{61}$$

$$\frac{t_m}{t_p} = \left(\frac{R_m}{R_p}\right)^2 \tag{62}$$

Substitution of equations (50) and (51) into equation (23) gives:

$$r^* = \frac{r}{R} \tag{63}$$

or

$$\frac{r_m}{r_p} = \frac{R_m}{R_p} \tag{64}$$

Equation (64) has significance in that some value may be chosen for the radius ratio to be substituted into other modeling equations, i.e. $R_m/R_p = \frac{1}{10}$, etc.

The following forms for the similarity parameters have been obtained:

$$\frac{T_m}{T_p} = \left(\frac{L}{I^2 \text{ Res}}\right)_p \left(\frac{I^2 \text{ Res}}{L}\right)_m \tag{65}$$

$$\frac{t_m}{t_p} = \left(\frac{R_m}{R_p}\right)^2 \qquad\qquad (66)$$

$$\frac{r_m}{r_p} = \frac{R_m}{R_p} \qquad\qquad (67)$$

The (I^2 Res) term is somewhat ambiguous for modeling purposes, but appears only because internal generation is a result of electrical resistance heating. Equation (65) may be put in a simpler form by substituting Res = ρ_e L/A, where ρ_e is the resistivity and depends on the material and temperature. There are numerous tables available that give the resistivity of common metals and alloys. Making the substitution for Res in equation (65) gives.

$$\frac{T_M}{T_P} = \left(\frac{R^4}{I^2}\right)_p \left(\frac{I^2}{R^2}\right)_m \qquad\qquad (68)$$

Equation (68) assumes that the resistivity for model and prototype are equal and that ρ_e = Res A/L accurately defines the resistivity. Tne experimental program showed the actual resistivity to be approximately ten per cent less than the theoretical resistivity defined by the ρ_e equation. This fact must be considered when equation (68) is used, plus the fact that if model and prototype are not fabricated from the same piece of stock the resistivities will differ slightly even if the model and prototype are made of the same material.

The final forms for the similarity parameters are as follows:

$$\frac{T_m}{T_p} = \left(\frac{R_p}{R_m}\right)^2 \left(\frac{I_m}{I_p}\right)^2 \qquad (69)$$

$$\frac{t_m}{t_p} = \left(\frac{R_m}{R_p}\right)^2 \qquad (70)$$

$$\frac{r_m}{r_p} = \frac{R_m}{R_p} \qquad (71)$$

A group of parameters were derived using equation (35), (36), and (41), since the radiation group was not included in the derivation above. The similarity parameters derived in this case gave reasonable results, but the results were not as accurate as those obtained by using equations (69), (70), and (71).

In most thermal modeling endeavors, the model to prototype ratio of the various parameters has a known constant value. This is particularly true for the dimensions of radius, length, etc. Experimental knowledge of a model and intuition assist the investigator in choosing the value of this model to prototype ratio.

For the rods tested in this investigation, the ratio (r_m/r_p) was known without making use of the scaling laws. Since radial heat conduction and surface radiation were the only modes of heat transfer involved in testing the rods, the lengths of the rods were arbitrarily selected. As stated previously, the procedure was to test a model, and predict the power input for the prototype that would give $(T_M/T_p) = 1$ at homologous

29

points along the surface of the rods. If this predicted power input

produced the desired temperatures, then the similarity parameters were

known to be valid. The time scaling term in equation (70) could then be

used to plot curves of temperature vs. time for the prototype and model

to further validate the similarity parameters, as shown in Chapter VI.

The curves should fall upon each other if the parameters are valid.

CHAPTER IV

TEST MODELS

The verification of the modeling criteria for a conduction-radiation
model was accomplished by using metal rods, and this design was chosen
for several reasons. The selection process was somewhat limited due to
problems in having the test sections fabricated within a given time peri-
od. The time factor also made it impossible to choose test sections that
would lead to extremely lengthy theoretical work in developing the modeling
criteria. Consequently, a solid rod was chosen as the most practical test
design to check the validity of thermal modeling criteria.

The solid rod met the requirements of giving one-dimensional (radial)
heat conduction under transient conditions. The rod surfaces were finished
at the same lathe speed to insure uniform and homologous surfaces on all
test sections, which in turn insured uniform radiation from the rods. With
the proper surface finishes it was then possible to achieve temperature con-
sistency at each point where the thermocouples were attached to the rods.

Two prototypes and two scaled models were constructed in order to
check the validity of the modeling criteria. The models and prototypes
were constructed from titanium alloy Ti-6AL-4V and type 304 stainless steel.
Tables 1 and 2 give the actual dimensions of the prototypes and models used
in the experimental phase of the program.

Each of the rods was threaded approximately 0.50 inches on the ends
so that the electrode terminal lugs could be firmly connected to the rods.

TABLE 1

MODEL DIMENSIONS

Model	Length L (in)	Diameter D (in)
Titanium	18.0	0.255
St. 304	24.0	0.2496

TABLE 2

PROTOTYPE DIMENSIONS

Model	Length L (in)	Diameter D (in)
Titanium	24.0	0.300
St. 304	24.0	0.374

A "snug" connection was necessary to assure proper conduction of current through the rods. Other techniques of attaching the electrodes were tried, but these were found to be far too awkward and inefficient in that extreme heating often occurred at one end of a rod.

As stated above, two electrical leads or electrodes were used to supply electrical power to the rods. The technique employed in sizing these leads is discussed in detail in Appendix A. One electrode was connected to each end of the rods. Two 20AWG copper leads (enamel coated) were also connected to each end of the rods to measure the electrical potential. The smaller leads were tightened around the threads by using pliers, and brass nuts were then screwed against the lead wires, which in turn pushed the wire firmly against the threads at the end of the rods. Following this the larger electrodes were attached to the rods. The ends of the electrodes were polished and were looped to fit the rod diameters. The electrode loop was slipped on the rod, and a nut screwed behind the loop forced it against the lead wire nut making an excellent electrical connection.

The thermocouples used were 30AWG copper-constantan, and the thermo-couple junction was made by soldering the wires together. This junction was then shaped to fit the curvature of the test section. The thermo-couple junction and lead wires were kept in place by using Devcon cement in the early stages of the experiment. However, this proved to be a poor technique and spot welding was used. Spot welding eliminated the possi-bility of the beads popping free of the rod during the test run, and minimized the response of the bead to voltage potential instead of

temperature at the various power settings.

All thermocouple wires and the lead wires used to measure electrical potential were polished twelve inches from the point where they left the system. These wires were then extended and soldered to a junction plate kept inside the vacuum chamber. This junction plate was used to facilitate the changing of test models. The wires were extended from the junction plate to feed-throughs located in the chamber wall. All thermocouples were checked on a Leeds and Northrup potentiometer before a model or prototype was put into the chamber to prove them functional.

Five thermocouples were attached to each of the models and prototypes. These were located at 16.66 per cent, 33.33 per cent, 50.0 per cent, 66.66 per cent, and 83.33 per cent of the rod length, measured from one end of the rod.

After the electrodes, electric potential leads, and thermocouples were attached to a rod, it was spray painted with a flat black paint, (Velvet coating 101-C10 by 3M) to a mean thickness of approximately 0.003 inches. Nylon cord was then tied to the ends of the rods, and they were hung in the center of the vacuum chamber.

CHAPTER V

EXPERIMENTAL PROGRAM

In order to verify the modeling criteria developed in Chapter III, the models and prototypes described in Chapter IV were tested inside a space simulation chamber. The modeling criteria were used to predict the thermal behavior performed on the geometrically similar designs. The chamber provided the necessary low temperature-low pressure environment so that an accurate prediction of the energy exchange between the rods and the surroundings could be made.

The space simulation chamber was a standard piece of test equipment located at NASA's Mississippi Test Facility. The chamber was a Murphy-Miller high vacuum altitude test chamber made of stainless steel. It was forty-seven inches in diameter by sixty inches long less shelf height of four inches, and had one removable stainless steel flange. The test chamber was connected to a diffusion pump and roughing pump for producing high vacuums to one-half micron absolute pressure. The chamber was also equipped with feed-throughs for copper-constantan thermocouples, potential leads, liquid nitrogen, and electric power.

Since it was necessary to obtain a low temperature environment, a liner was placed in the main chamber. The liner shell was constructed of stainless steel and was fifty-eight inches long and forty-three inches in diameter. The shell was spiral wrapped with five-eighth inch diameter copper tubing which carried the liquid nitrogen. At one end of the liner

was an optically tight baffle and at the other end was a removable flange. A liquid level controller was used in conjunction with a solenoidally operated valve to control the flow of nitrogen and to insure that liquid was in the tubing at all times during a test. The inner wall of the liner was coated with a flat black paint (velvet coating 101-C10) in order to insure surfaces with high and uniform values of emittance and absorptance. The outer wall of the liner and inner wall of the chamber were covered with foil to reduce the heat loss from the chamber. In order to minimize conduction from the outer chamber wall to the liner, it was necessary to support the liner on four adjustable legs. A schematic of the test facility is shown in Figure 3, and a photograph of the overall vacuum system is shown in Figure 4 (the fluid injection system shown in Figure 4 was used for experiments other than thermal modeling at MTF).

The inner wall of the liner reached $-300°F$, and the outer wall of the liner reached $-275°F$ using liquid nitrogen. Figures 5 and 6 show the LN_2 lines as well as hot water lines used to return the chamber temperature to room temperature as quickly as possible after a test run.

To perform the transient tests on the rods, each rod was located centrally within the liner. The horizontal position of the rods was attained by extending nylon cords from hooks at the top of the liner to the ends of the rods. The nylon cord was very long in comparison to its diameter to minimize conduction losses. A photograph of the rod position is shown in Figure 7.

The thermocouple output was obtained by using eight strip-chart recorders. Five recorders provided the test rod temperatures, a recorder
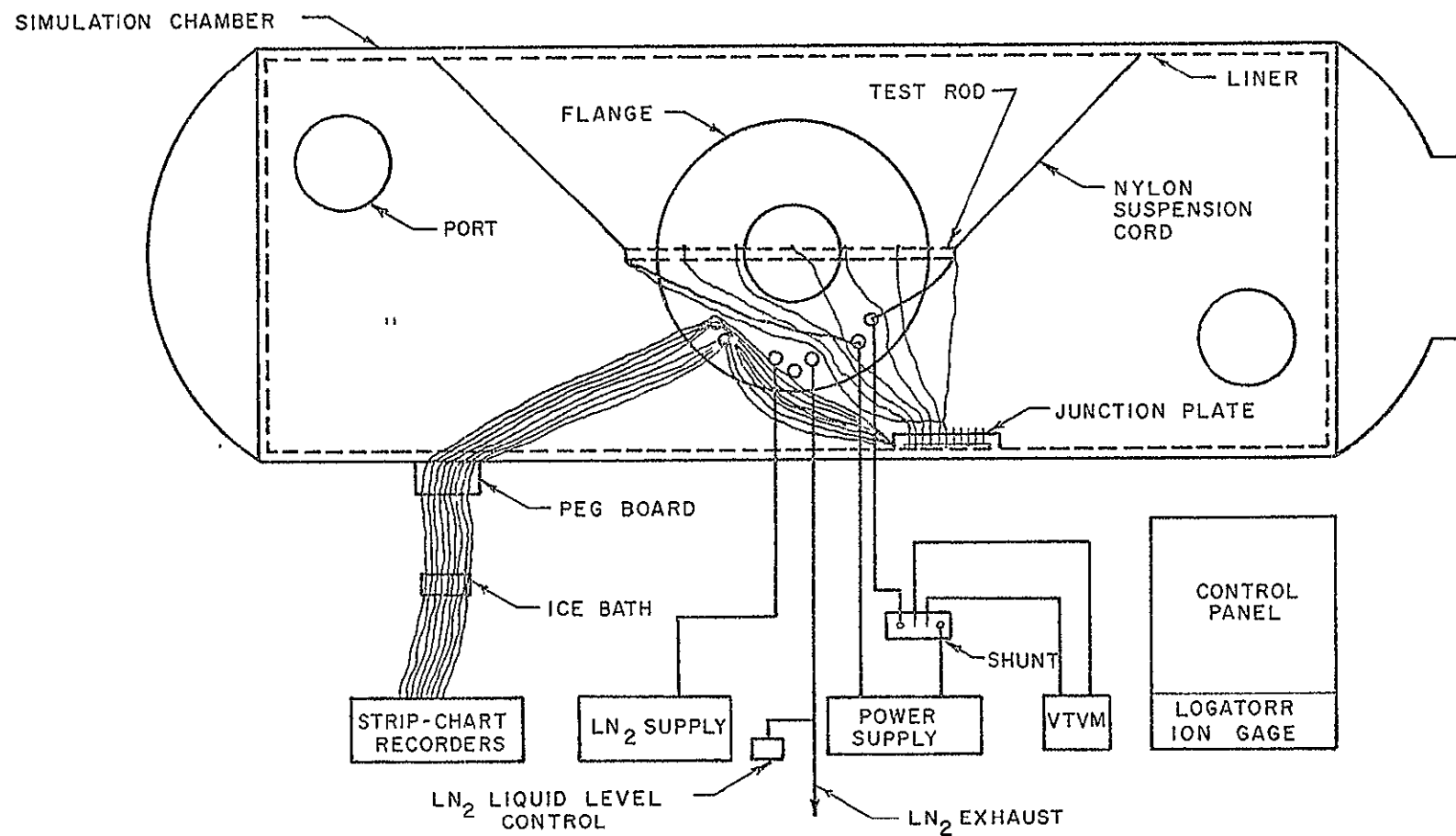
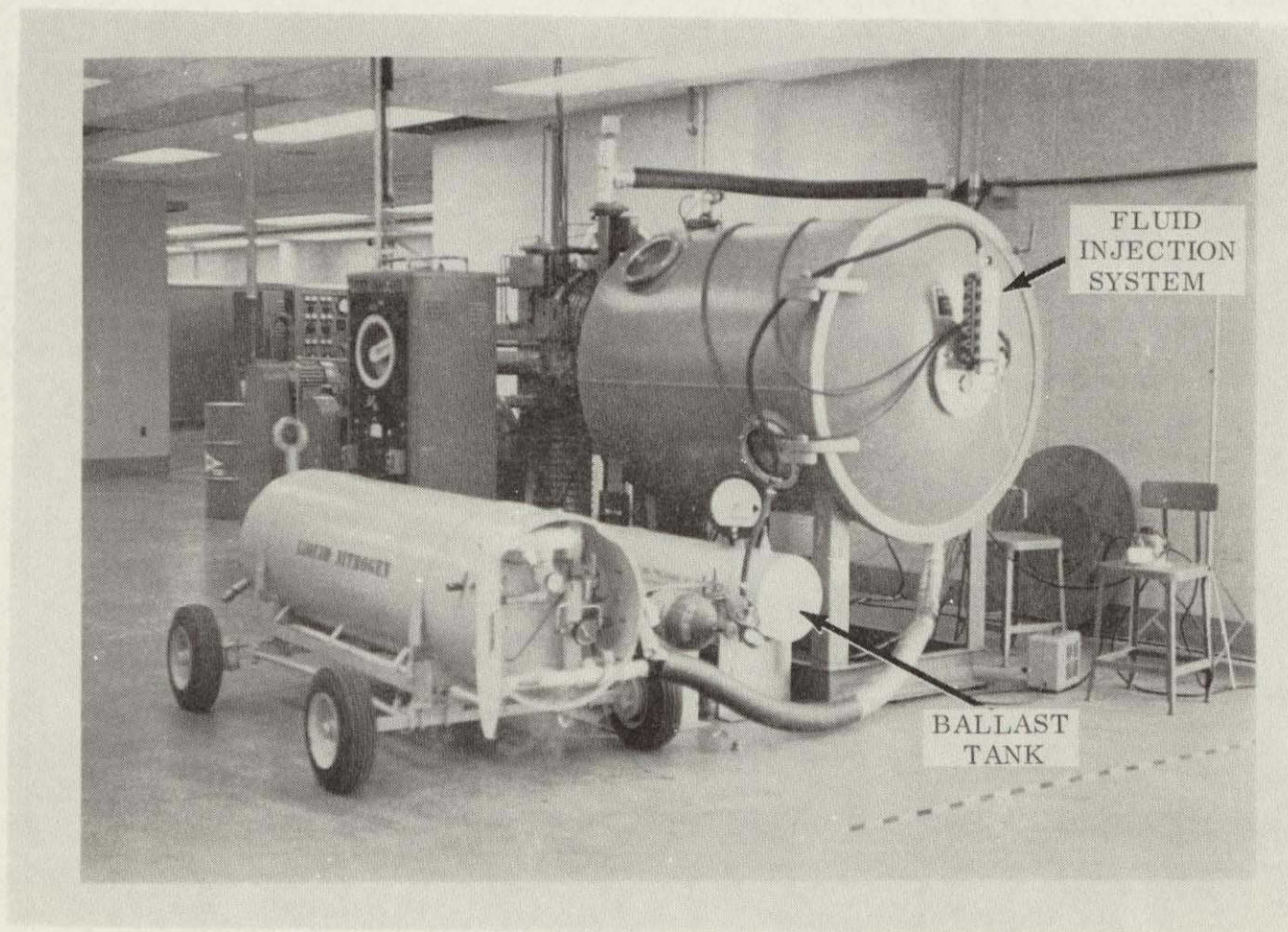SCHEMATIC OF TEST FACILITY

Figure 3
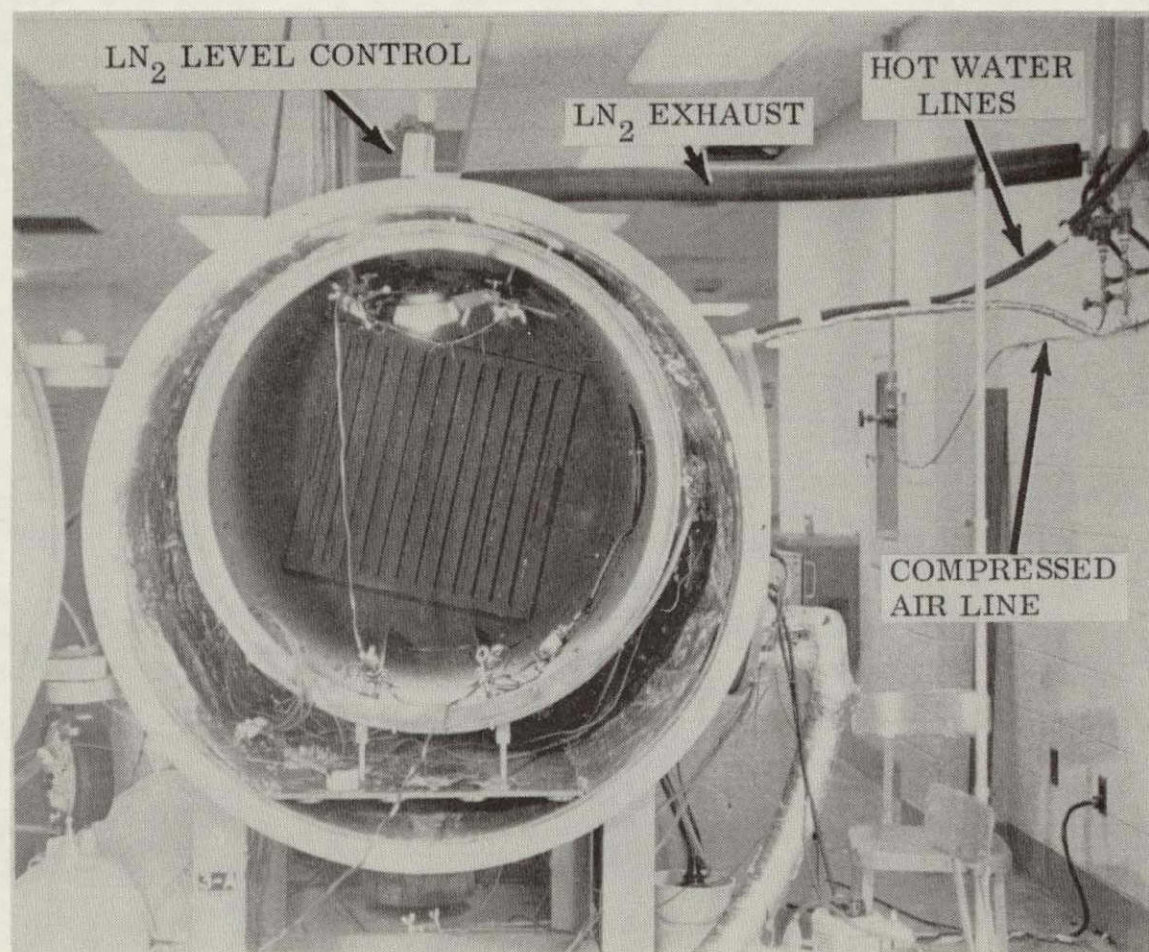
Figure 4

Overall View of Test Apparatus

LN$_2$ LEVEL CONTROL

LN$_2$ EXHAUST

HOT WATER LINES

COMPRESSED AIR LINE

Figure 5
End View of Vacuum Chamber
Showing Cryogenic Liner

THERMOCOUPLE
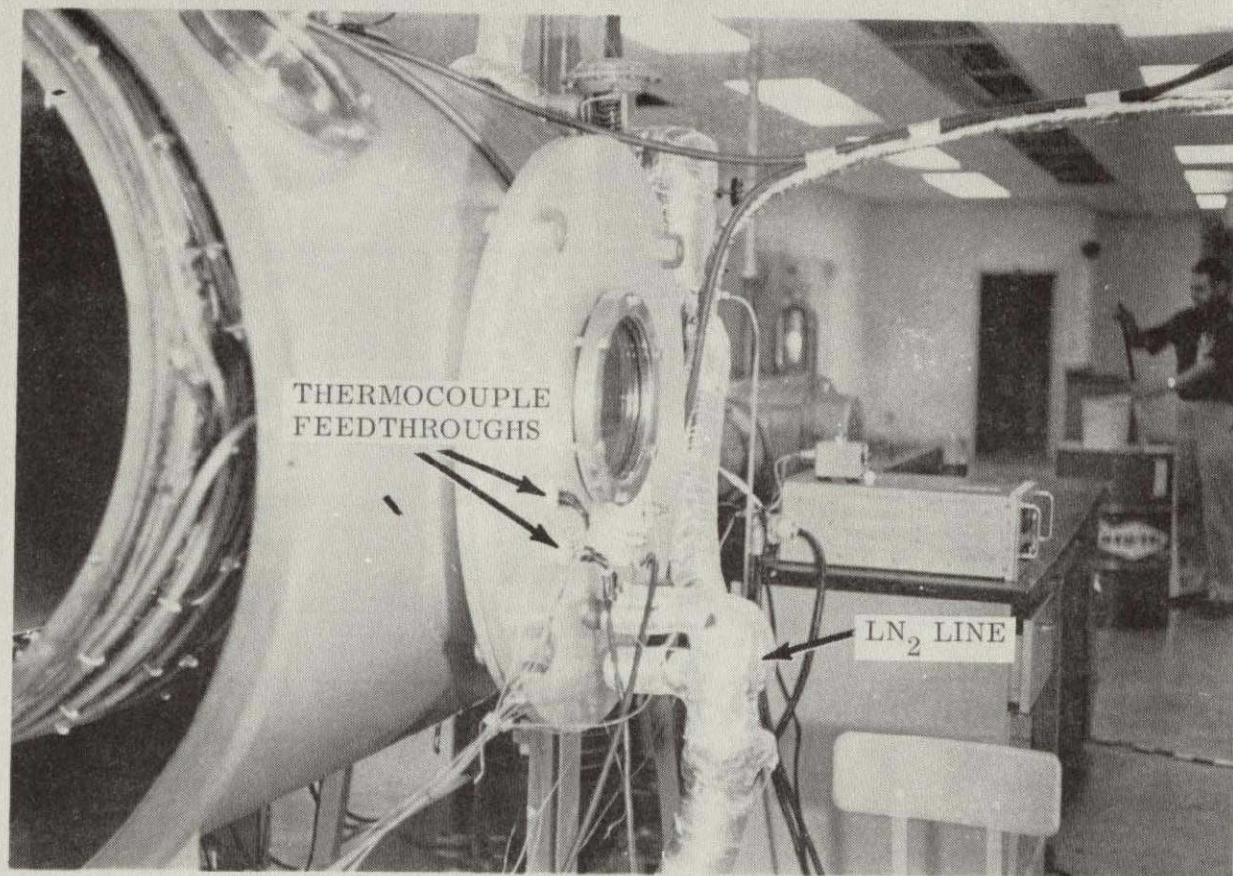FEEDTHROUGHS

LN$_2$ LINE
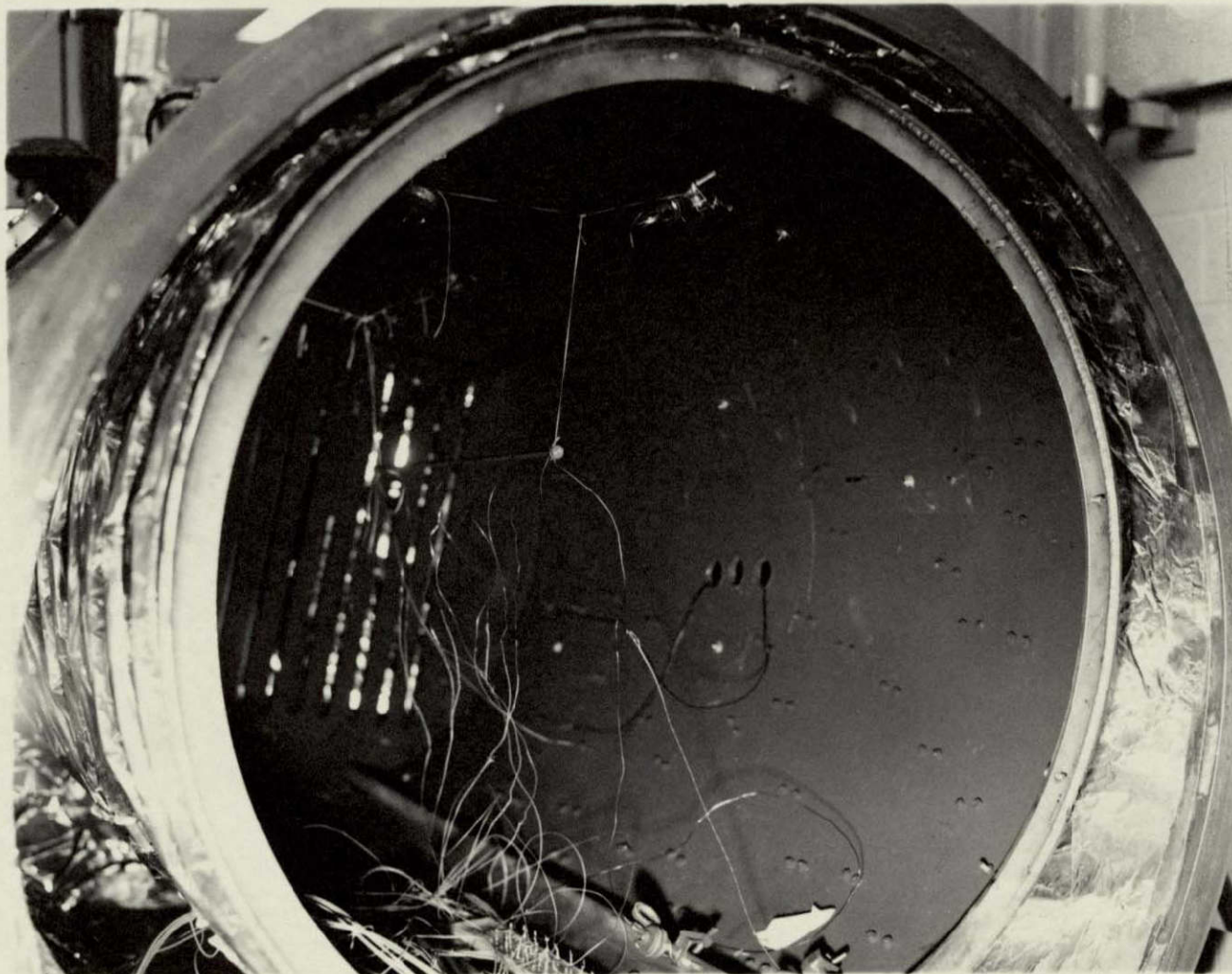
Figure 6

Flange Plate

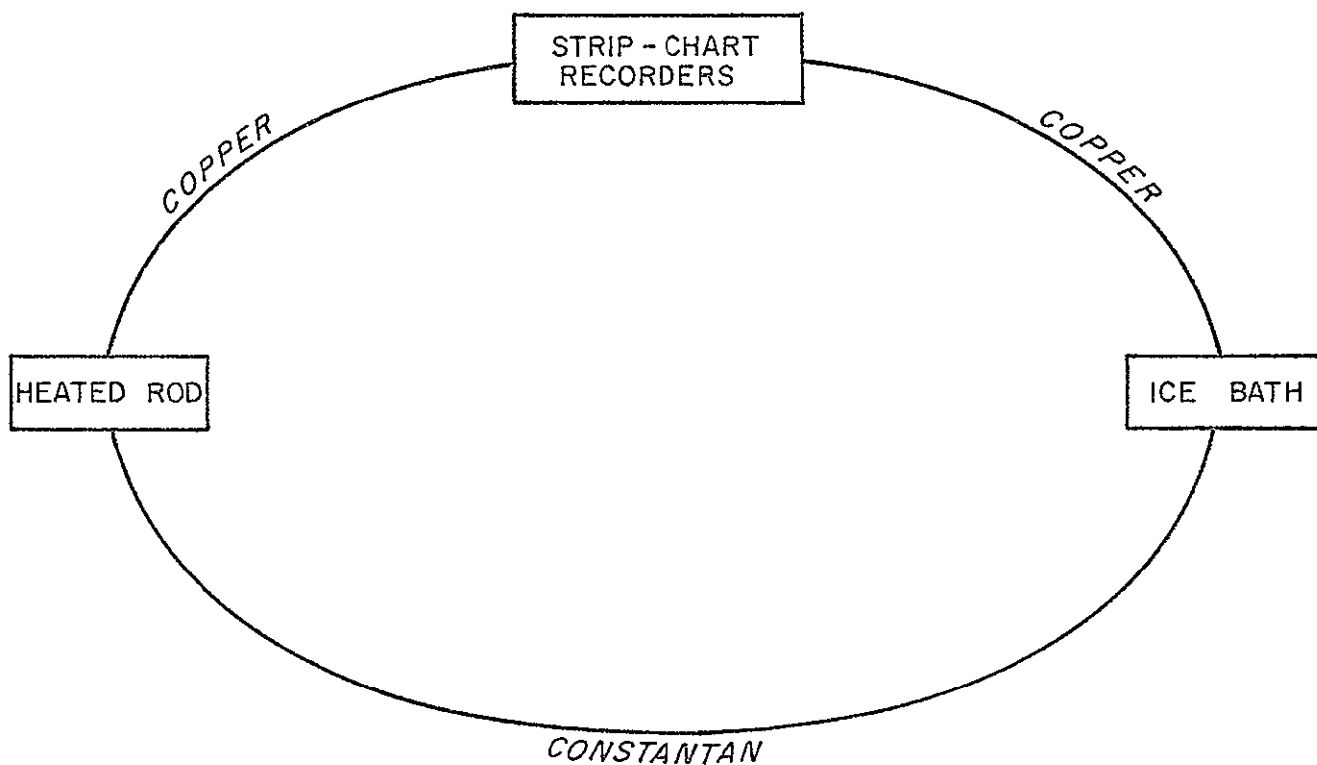Figure 7

Rod Position in Vacuum Chamber

gave the power lead temperature, another recorder provided the inside liner temperature, and the remaining recorder provided a measure of the current input to the rods. The recorders were calibrated with a Leeds and Northrup portable potentiometer with a reference temperature of 32°F. During the tests, the thermocouple reference function was maintained at 32°F with an ice bath. Figure 8 shows the path followed by the thermocouples in reference to the strip chart reocrders, i.e., the thermocouple circuit. Appendix B explains the procedure used to convert millivolt readings from the recorders to temperature readings.

Before each test run the test rod was exposed to a vacuum environment at ambient temperature for a period of time. At this condition the output of all thermocouples was within $\pm$ 0.20 millivolt of each other. It was therefore reasonable to assume that temperatues were measured to an accuracy of approximately + 1.00 during the test.

For transient testing, a D-C power supply could be hand controlled to within $\pm$ 1 millivolt during test runs.

Current input to the rods was determined by measuring the millivolt drop across a calibrated shunt in series with the rods, using a vacuum-tube voltmeter. The VTVM was also used to measure the potential drop across the rods by making use of the leads attached to the rods for this purpose.

The voltage drop and current input determined from the VTVM were used to check the resistance change of the rods as the power input was increased. The resistance was found to be relatively constant in the zero to one-hundred degrees Fahrenheit range used during the test.

THERMOCOUPLE   CIRCUIT

Figure 8

Time measurement was accomplished by the time marker on the strip chart recorders. The error involved was negligible.

The pressure inside the vacuum chamber was measured with a logatorr ion gage. The pressure was approximately 1×10^{-6} torr.

After a test rod was installed within the liner, the thermocouples were connected to a junction plate, which in turn was connected to the power feed-throughs, the liner flange was installed, and the system was then ready for a test run. Pump-down was accomplished and the thermocouples were checked for equality of output. When the chamber pressure reached approximately 1×10^{-6} torr, liquid nitrogen flow was started. After approximately three hours, complete cool-down was achieved.

The copper tubing around the liner was maintained full of liquid nitrogen by a liquid level control system. The models and prototypes were protected from temperature extremes by adjusting the power input to the rods during the cool-down period.

The input to the rods was set at a desired value and temperature recorded until steady conditions were established. Then the potential drop, current input, and temperature at the five thermocouple locations on the rod were recorded. A difference of approximately one-half degree per hour implied steady conditions.

At this point, the power input was changed to a higher value and the temperatures and times were recorded until new steady conditions were reached.

CHAPTER VI

EXPERIMENTAL RESULTS AND CONCLUSIONS

Transient Results

The experimental phase of the thermal scale modeling investigation was conducted using the facility described in Chapter V. The transient testing included testing of two prototypes and two models. The first test run was made using a titanium model and prototype, with $R_M/R_P = 0.825$. Secondly, the stainless steel model and prototype were tested, with $R_M/R_P = 0.66$. Each test was conducted in accordance with the procedure described in Chapter V.

As stated in Chapter IV, the early part of the experiment was plagued by heat loss at the ends of the rods where the power leads were connected. Several test runs were made in an effort to eliminate this problem, and as stated in Chapter IV, a reliable technique was found. Several other miscellaneous problems were encountered in the earlier runs, but these were eventually eliminated.

The energy input to the models was arbitrarily selected and a correspondingly scaled input was used for the prototypes according to the value predicted from equation (59). Temperatures were measured following the test procedures described in Chapter V. Tables III and IV show the scaled input values for the prototypes and the resulting temperatures obtained.

Figures 9 and 10 present the measured temperature-time data for the two models and the corresponding time-scaled temperature-time data for

TABLE III

TITANIUM RESULTS
EXPERIMENTAL DATA

	INITIAL TEMPERATURE		FINAL TEMPERATURE	
	Model	Prototype	Model	Prototype
I (AMPS)	10.050	12.75	12.50	15.85
E (VOLTS)	0.231	0.286	0.289	0.360
P (WATTS)	2.322	3.646	3.612	5.698
TC1 (°F)	11.80	8.00	58.00	53.00
TC2 (°F)	11.00	11 00	58.00	59 20
TC3 (°F)	12.10	12.00	59.50	59.00
TC4 (°F)	11.50	10.60	59.40	58.00
TC5 (°F)	12.00	6.70	55.70	56.60

TABLE IV

STAINLESS STEEL RESULTS
EXPERIMENTAL DATA

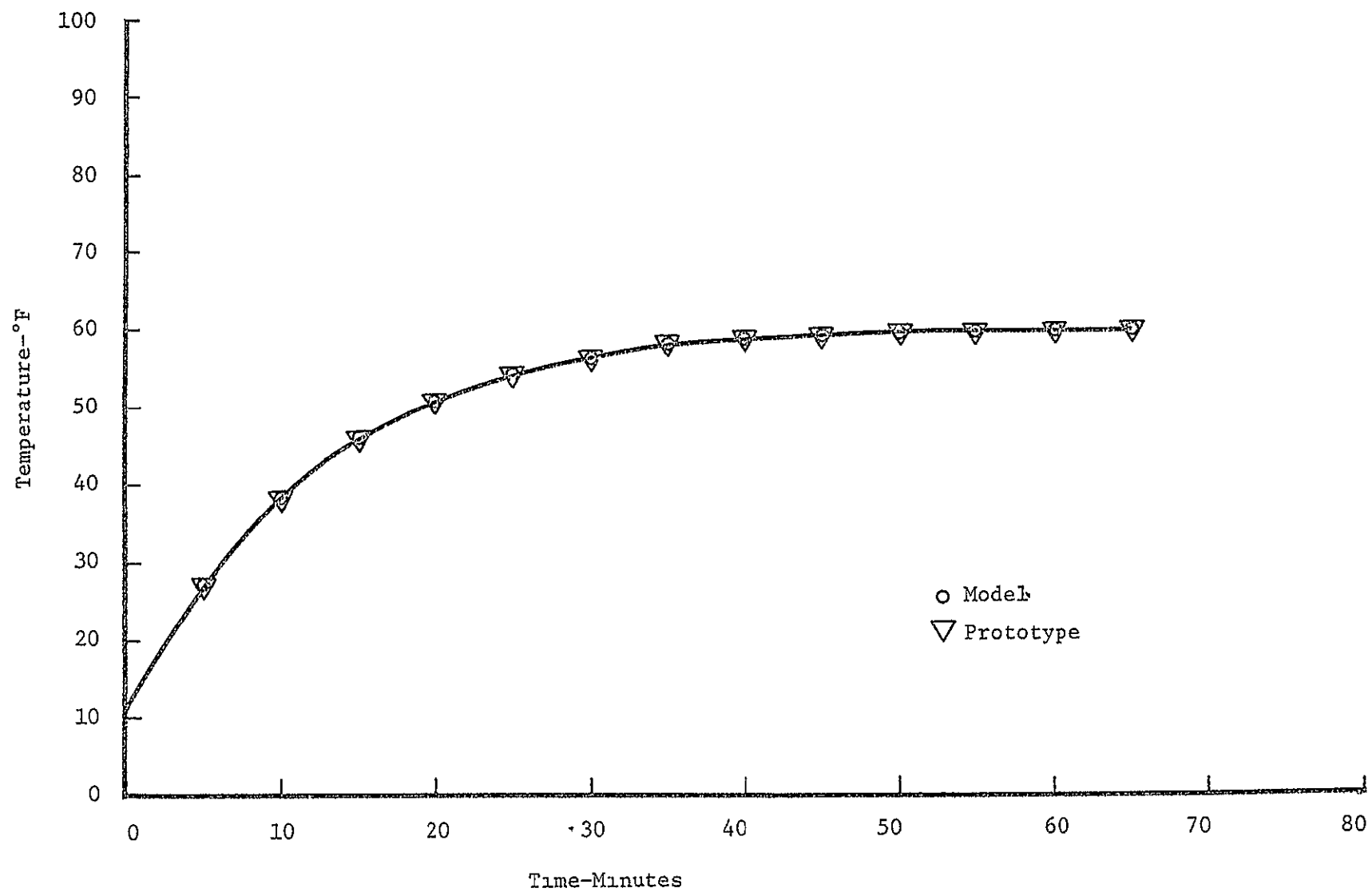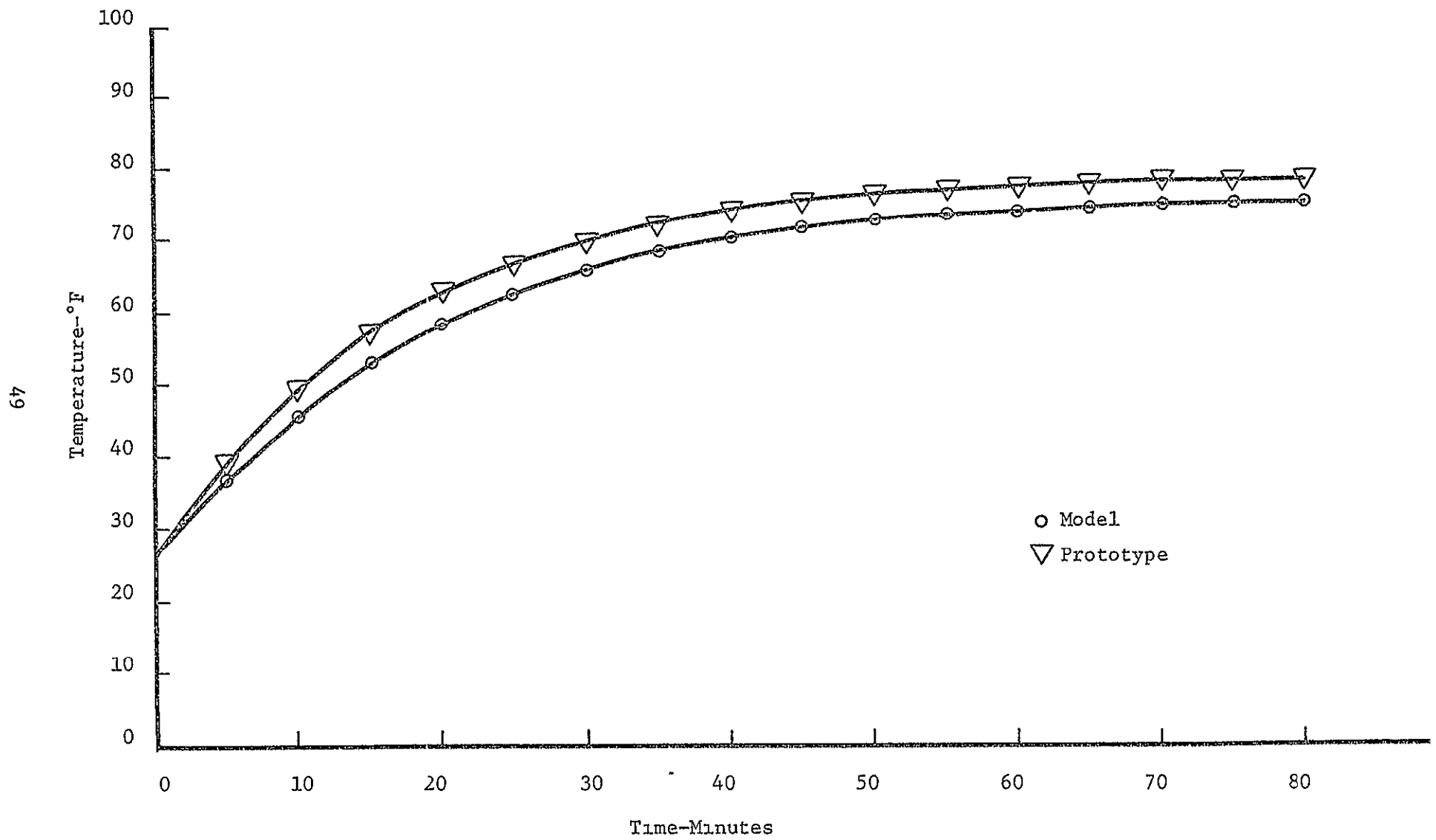|	INITIAL TEMPERATURE		FINAL TEMPERATURE	
	Model	Prototype	Model	Prototype
I (AMPS)	15.30	29.60	18.65	36.30
E (VOLTS)	0.236	0.176	0.280	0.216
P (WATTS)	3.611	5.224	5.222	7.859
TC1 (°F)	26.10	27.50	76.70	78.00
TC2 (°F)	25.50	27.00	74.00	77.50
TC3 (°F)	26.00	26.50	75.00	76.00
TC4 (°F)	24.80	26.00	72.80	75.40
TC5 (°F)	25.00	25.00	74.00	76.40

Figure 9

Temperature vs Time-Titanium

Figure 10

Temperature vs Time-Stainless Steel

the prototypes. Generally, there was excellent prediction of prototype

temperatures from model data. The titanium results agreed perfectly, and

the largest average absolute error for stainless steel model and proto-

type was three and one-half degrees. A discussion of the errors involved

is included in the following section of this chapter.

Miller (21) conducted research with a solid cylindrical design made

of two dissimilar materials. An interesting comparison exist between the

similarity parameters Miller obtained and those obtained in this investi-

gation. Some of the parameters he derived (neglecting property variations)

were as follows:

$$\frac{q_m}{q_p} = \frac{(RL)_m}{(RL)_p} \tag{72}$$

$$\frac{T_m}{T_p} = 1 \tag{73}$$

$$\frac{t_m}{t_p} = \frac{(\rho cr)_m}{(\rho cr)_m} \tag{74}$$

These parameters were used for steady and transient predictions Since

$(\rho c)_m = (\rho c)_p$ equation (74) reduces to.

$$\frac{t_m}{t_p} = \frac{R_m}{R_p} \tag{75}$$

The discovery was made that Miller's equation (72) predicted the same

power settings as did equation (59), using the conversion 0.293 watts/btu/hr.

Consequently, temperature-time curves were drawn using Miller's time-scaling equation (75). The results are shown in Fiugres 11 and 12, and indicate that use of equation (75) yields reasonably accurate results. Comparison of Figures (8), (9), (10), and (11) show that prototype temp-ratures are slightly higher when time-scaled using $t_p = t_m (\frac{R_p}{R_m})^2$ as com-pared to Miller's expression $t_p = t_m (\frac{R_p}{R_m})$.

Error Analysis

Some consideration was given to instrumentation errors in Chapter V. This section will discuss possible effects caused by such factors as in-correct power input to the model, energy losses through thermocouple leads and power leads, and variation of thermal properties.

The power input to the models and prototypes was generally different than that required by the similarity parameters. Several test runs were made with each model and prototype, and the resulting quantity of data provided a means of determining what effect slight power differences had on the rod temperature. The largest difference between actual power input and the input required by the parameters was +0.05 watts for the stainless steel prototype. This led to a +1 degree error, approximately. The input power to the titanium model and prototype was extremely close to that which the parameters required, which implied a negligible error

Miller (21) discussed a means of estimating thermocouple loss. The thermocouple leads were considered to be infinitely long pin fins with a known root temperature, and with radiation heat transfer from the fin surface. The differential equation that describes this situation is·
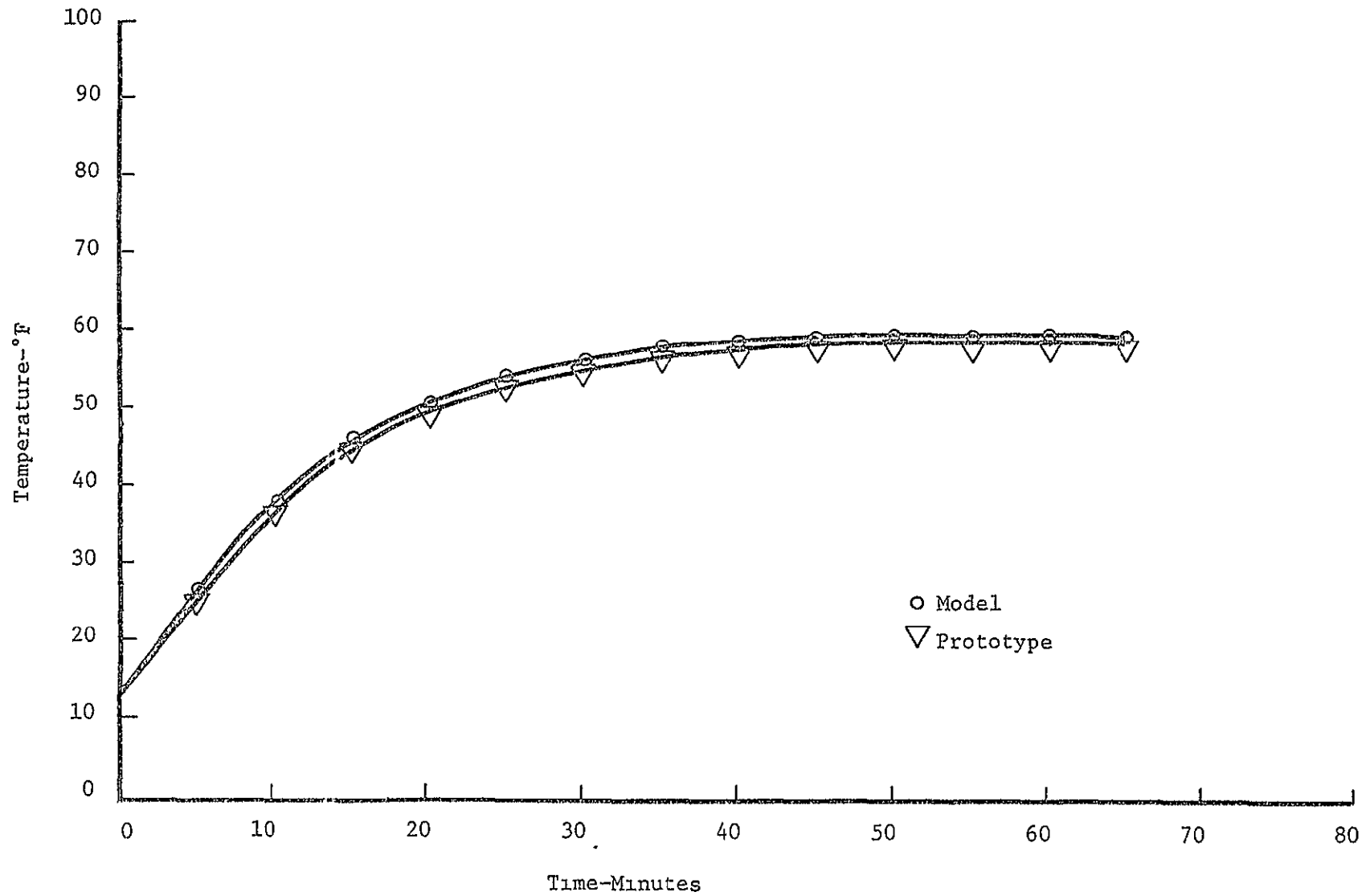
51

Figure 1ĭ

Temperature vs Time—Titanium
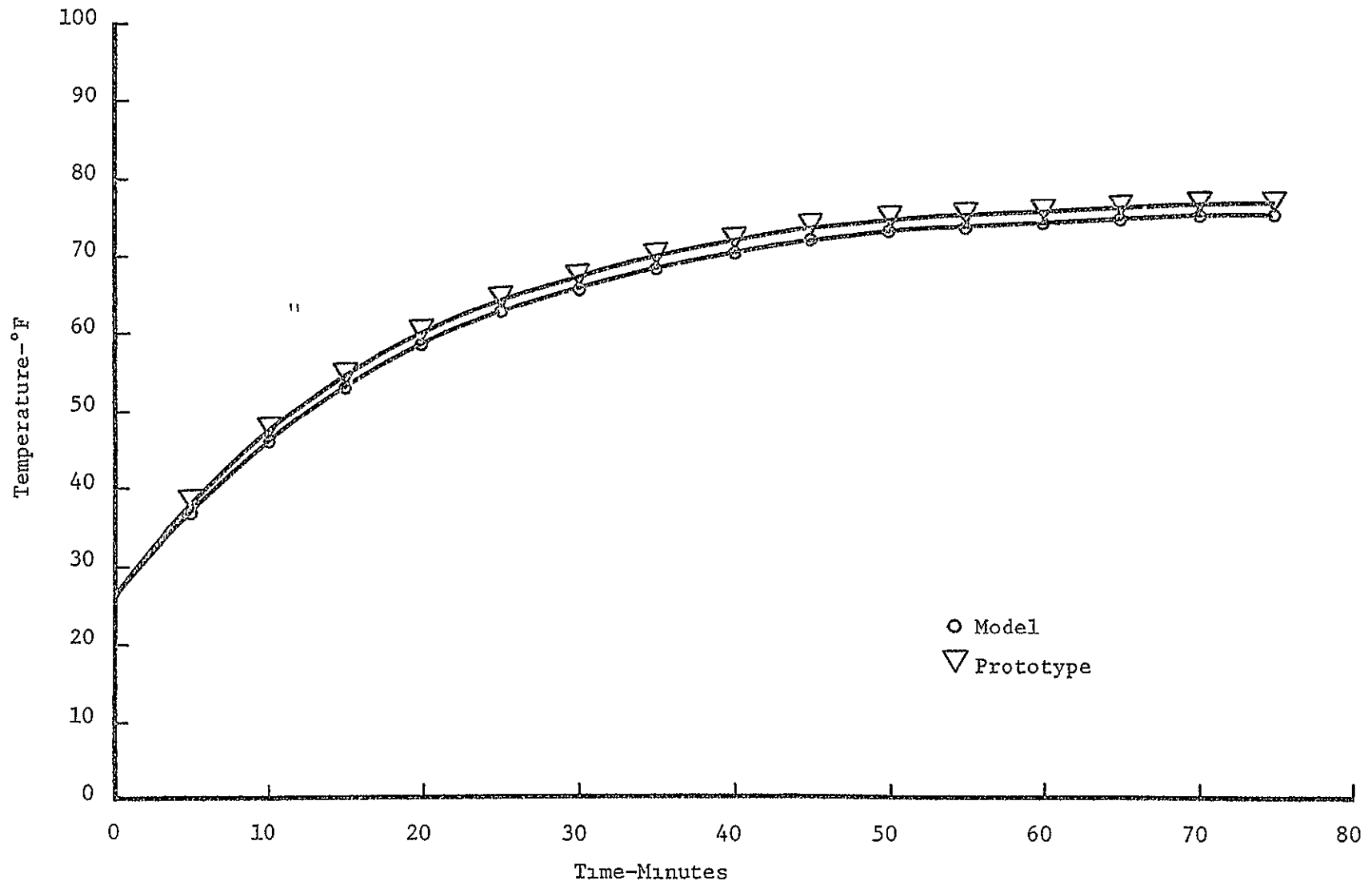Miller's Approach

52

Figure 12
Temperature vs time-Stainless Steel
Miller's Approach

$$kR \frac{d^2T}{dx^2} = 2\varepsilon\sigma T^4 \qquad (76)$$

This equation may be integrated once with respect to x to yield the heat transfer rate at the root of the fin, the desired quantity.

$$q_o = -kA_n\left(\frac{dT}{dx}\right)_{x=0} = \left[\frac{4}{5} \Pi^2 R^3 k\varepsilon\sigma (T_o^5 - T_\infty^5)\right]^{1/2} \qquad (77)$$

The wire radii were known from tabulated values for 30 gage wire. Thermal conductivities of 220 BTU/hr – ft – °F and 14 BTU/hr – ft – °F for copper and constantan, respectively, were used in calculations. The surface emittance values were estimated for the polished wires as 0.05 for copper and 0.10 for constantan. Measured values were used for T_o and T_∞ was assumed to be 150°R, the boiling temperature of liquid nitrogen. The total thermocouple loss was less than one per cent.

Losses through the nylon support lines were considered to be negligible.

The problem of power lead loss (or gain) was eliminated by scaling the leads using the technique in Appendix A. A dramatic temperature drop from the center to the ends of the rods was observed when oversized leads were used. The reverse trend was present when undersized leads were used and acted as heat sources for the rods.

In the derivation of the similarity parameters, it was assumed that model and prototype were constructed of the same material, which implies that thermal conductivity and specific heat were equal in model and prototype. Since the percentage of alloying elements for a particular material

54

is not the same for each batch from a particular manufacturer or for materials with the same alloy specifications from different manufacturers, there was a possibility that model and prototype had slightly different thermal properties.

Miller (21) assumed that material properties varied with temperature according to the relationships·

$$k = k_o T^a \tag{78}$$

$$c_p = c_{po} T^b \tag{79}$$

The effects of the variation, from lot-to-lot, of the conductivity and specific heat on the value of the modeling parameters was illustrated by assuming that the exponents in his power law equations were the same for both model and prototype which determined the effect of the variations of k_o and c_{po}. Miller found that a three per cent variation in k_o could cause a four percent variation in the input energy parameter, a three per cent variation in the temperature parameter. Comparison of resistance per foot data for models and prototypes indicated that a similar trend existed in this investigation.

CONCLUSIONS

The temperature-time data in Figure 8 and 9 verify the applicability
of thermal modeling to a transient system with internal generation. The
objective of the investigation was satisfied by experimental verification
of the analytically derived similarity parameters. The development of a
power lead scaling technique and presentation of error analysis techniques
should be useful in future thermal modeling endeavors.

APPENDIX A

TECHNIQUE OF SIZING POWER LEADS

TECHNIQUE OF SIZING POWER LEADS

The problem of heat loss due to conduction at the ends of the
prototypes and models proved to be a problem of significant magnitude
during the experimental phase of the investigation. After many test
runs, it was determined that the size of the power leads connected at
each end of a model or prototype was the chief source of this problem.
If the leads were much larger in diameter than the test rods, they
served as heat sinks at the rod ends. However, undersizing the leads
tended to reverse the situation, and a heat source was created at the
rod ends. It was thus necessary to develop a technique of scaling the
power leads for each test rod in such a way that the leads would not
serve as a heat sink or heat source.

The power supplied to a test rod can be expressed as:

$$P = I^2 R \tag{1}$$

Since the same current passes through the leads as through the rod,
the following equation must hold:

$$\frac{P_L}{P_R} = \frac{R_L}{R_R} \qquad = \tag{2}$$

The above resistances have the unit ohms per foot of length.

The power supplied to each test rod is dissipated by radiation at
the surface of the rod. It is evident, then, that the watts of power
supplied can be expressed in terms of heat radiated. The ratio of the
heat radiated from the lead and rod is given by:

$$\frac{q''_L}{q''_R} = \frac{\sigma_L \varepsilon_L T_L^4 A_{sL}}{\sigma_R \varepsilon_R T_R^4 A_{sL}} \tag{3}$$

The emissivity terms were made equal by painting the leads black.
This had the effect of keeping the lead cooler, since it closely
approached being a perfect radiator. Conversely, polishing the leads
tended to keep them warmer. For steady state temperature between the
leads and rod, equation (3) becomes:

$$\frac{q''_L}{q''_R} = \frac{A_{sL}}{A_{sR}} \tag{4}$$

Since heat radiated and power are related by a constant conversion,
(.293 watts/BTU/hr), equations (2) and (4) can be related to give

$$\frac{A_{sL}}{A_{sR}} = \frac{R_L}{R_R} \tag{5}$$

Equation (5) reduces to.

$$\frac{D_L}{D_R} = \frac{R_L}{R_R} \tag{6}$$

The resistance per foot of length of the rod can be found by running
a known current through the lead and measuring the voltage drop with a
voltmeter. The application of Ohm's law will then give the test rod
resistance R_R. The diameter of the rod was already known, so, D_R/R_R may
be reduced to a constant C, and equation (6) becomes·

$$D_L = CR_L \tag{7}$$

Equation (7) is obviously linear.

To utilize equation (7), a plot of lead diameter in inches vs resistance in ohms per foot of length was made by using a table of the properties of copper wire. By picking several values of R_L in equation (7), it was possible to draw a straight line through the above mentioned curve, where the origin of this line began at $R_L = 0$ and $D_L = 0$. This starting point was found by simply substituting $R_L = 0$ into equation (7), which resulted in $D_L = 0$. The intersection of the curve and the line given by equation (7) gives the proper diameter to use for each test rod.

APPENDIX B

Conversion of Millivolt Readings
to Temperature Readings

Conversion of Millivolt Readings
to Temperature Readings

Some explanation is in order concerning the procedure followed in
converting the millivolt reading from the recorders to temperature readings.
Holman (24) stated that it is common to express thermoelectric emf in terms
of the potential generated with a reference junction at 32°F. Standard
thermocouple tables have been prepared on this basis showing the output
characteristics of many common thermocouple combinations. Such a table
was used for the copper-constantan thermocouples utilized in this experiment.

A Leeds and Northrup 8690 potentiometer was connected directly to
each strip-chart recorder, and the slidewire scale setter was turned on
the potentiometer until the pointer on the strip-chart recorder was at
the zero point on the recorder paper. The strip-chart paper was divided
into one-hundred intervals. When the pointer was above the zero point
on the recorder paper, the millivolt reading on the potentiometer was
recorded. This procedure was followed in intervals of ten across the
recorder paper until the one-hundred intervals had been crossed. Then
the copper-constantan thermocouple table referenced at 32°F was used to
match the data in the table with the data recorded. It was found that
the recorders had a tolerance of ± 1.0 degree Fahrenheit. From the re-
corded data a plot of percent of millivolt range across recorder paper
vs. temperature was made as shown in Figure B-1. This curve was used
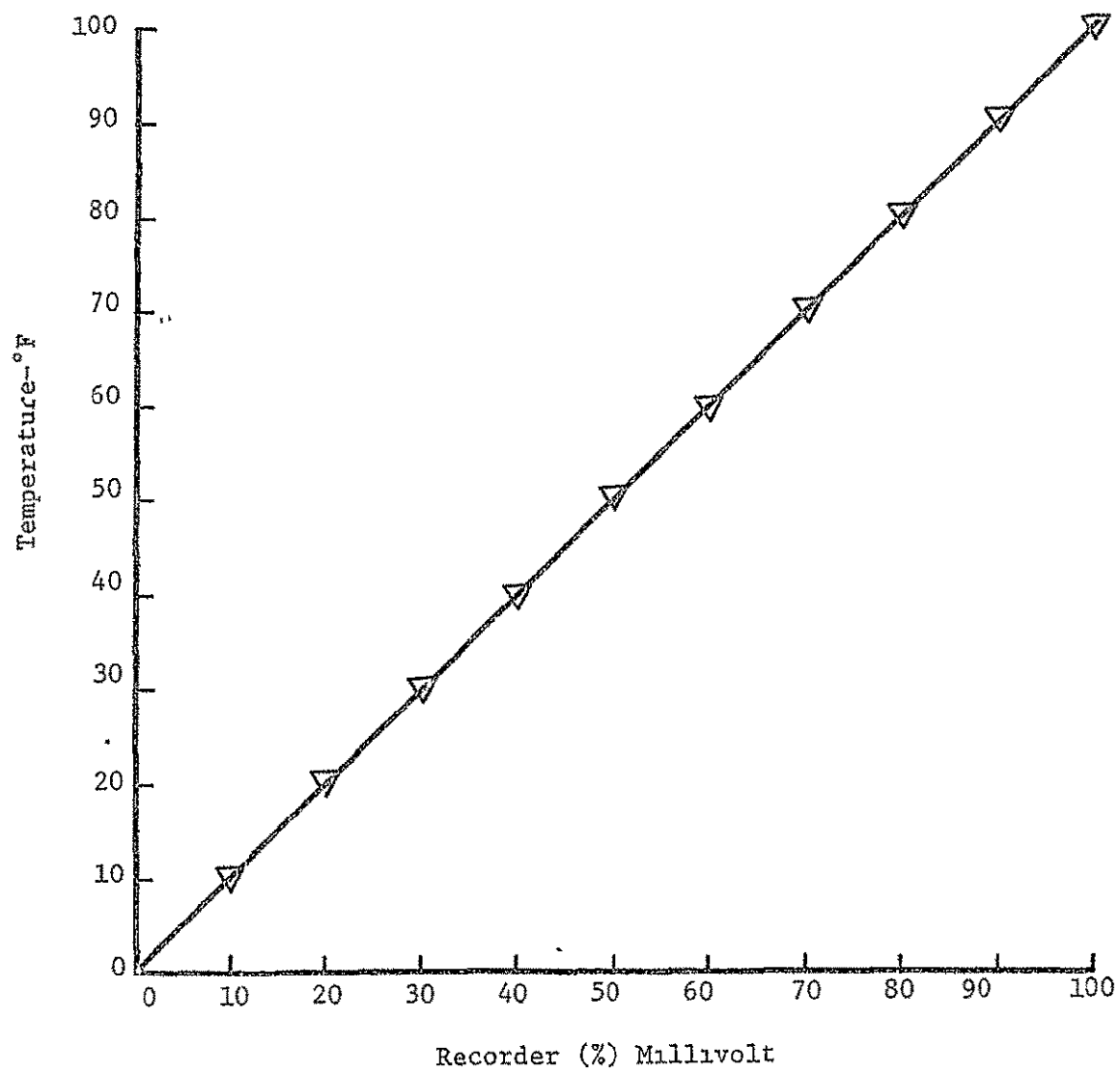to determine model and prototype temperature from the strip chart recorders.

Figure B-1
Temperature Range vs % Millivolt
Range on Strip-chart Recorder

REFERENCES

1. Vickers, J. M. F., "Thermal Scale Modeling". Astronautics and Aeronautics, pp. 34-39, May 1965.

2. Katzoff, S , "Similitude in Thermal Models of Spacecraft". NASA Tn-D-1631, April 1963.

3. Katz, A. J., "Thermal Testing". Space/Aeronautics (Aerospace Test Engineering-Part 2), pp. 30-34, October 1962.

4. Clark, L. G. and K. A. Laband, "Orbital Station Temperature Control". Astronautics, pp. 40-43, September 1962.

5. Wainwright, J. B., L. R. Kelly, and T. H. Keese, "Modeling Criteria and Testing Technique for the Simulation of Space Environments". Fourth Annual Symposium on Space Environment Sciences, pp. 257-263, April 1964.

6. Hrycak, P. and B. A. Unger, "General Criteria for Solar Simulation and Model Testing" Proceedings 1964 Annual Technical Meeting of the Institute of Environment Sciences, pp. 257-263, April 1964.

7. Jones, B. P., "Similitude Research in Space Vehicle Thermal Problems". Proceedings of Conference on Thermal Scale Modeling, NASA/OART, pp. 17-35, February 1964.

8. Jones, B. P., "Thermal Similitude Studies". J. Spacecraft and Rockets, 1, Nr. 4, pp. 364-369, July-August 1964.

9. Chao, B. T. and G. L. Wedekind, "Similarity Criteria for Thermal Modeling of Spacecraft". Journal of Spacecraft and Rockets, 2, Nr. 2, pp. 146-152, March-April 1965.

10. Fowle, A. A., F. Gabron, and Vickers, J. M. F., "Thermal Scale Modeling of Spacecraft: an Experimental Investigation". AIAA Space Simulation and Testing Conference, Pasadena, California, November 1964.

11. Vickers, J. M. F., "Thermal Scale Modeling: Basic Considerations". Jet Propulsion Laboratory Space Programs Summary IV, No. 37-18, 80-85, December 1962.

12. Watkins, J. R., "Thermal Similitude Using Brand's Theorem". Proceedings of Conference on Thermal Scale Modeling, NASA/OART, pp. 3-16, February 1964.

13. Matheny, J. D., "Thermal Design Studies". Final Report, Contract NAS8-5270, September 1965.

14. Folkmann, N. R., F. L. Baldwin, and J. B. Wainwright, "Tests on a Thermally Scaled Model STation in a Simulated Solar Environment". AIAA Thermophysics Specialist Conference, Monterey, California, Paper Nr. 65-658, September 1965.

15. Rolling, R. E , "Results of Transient Thermal Modeling in a Simulated Space Environment". AIAA Thermophysics Specialist Conference, Monterey, California, Paper Nr. 65-659, September 1965.

16. Rolling, R. E., "Thermal Modeling of a Truncated Cone in a Simulated Space Environment". AIAA Space Simulation Conference, Houston, Texas, September 1966.

17. Young, R. L. and Shanklin, R. V., "Thermal Similarity Study of a Typical Space Vehicle Element". Presented at the AIAA Aerospace Meeting, New York, New York, January 1966.

18. Gabron, F. and R. W. Johnson, "Thermal Scale Modeling of the Temperature Control Model of Mariner Mars 64". Reports on contract research by A. D. Little, Inc. for Jet Propulsion Laboratory, Pasadena, California. Phase IA, May 1964; Phase IB, July 1964; Phase II, January 1965.

19. Jones, B. P. and J. K. Harrison, "A Set of Experiments of Thermal Similitude". NASA TMX-53346, October 1965.

20. Adkins, D. L., "Scaling of Transient Temperature Distributions of Simple Bodies in a Space Chamber". Presented at the AIAA Termophysics Specialists Conference, Monterey, California, September 1965.

21. Miller, P. L., "Thermal Modeling in a Simulated Space Environment". Ph. D. Dissertation at Oklahoma State University, July 1966.

22. Shih, C., "Thermal Similitude of Manned Spacecraft". Presented at the AIAA Aerospace Sciences Meeting, New York, New York, January 1966.

23. Price, J. W., "A Thermal Scale Model with Experimental and Theoretical Results". George C. Marshall Space Flight Center, IN-P and VE-P-68-6, January 1968.

24. Holman, J. P., Experimental Methods for Engineers. McGraw-Hill Book Company, New York, 1966.

25. Murrill, P. W., R. W. Pike, and C. L. Smith, Formulation and Utilization of Mathematical Models, Louisiana State University Department of Chemical Engineering, copyright pending.

26. Kreith, Frank, Principles of Heat Transfer. International Textbook Company, Scranton, Pennsylvania, 1967.